



PCCP

**Computational predictions of metal-macrocycle stability constants require accurate treatments of local solvent and pH effects**

Journal:	<i>Physical Chemistry Chemical Physics</i>
Manuscript ID	CP-ART-02-2021-000611.R1
Article Type:	Paper
Date Submitted by the Author:	31-Mar-2021
Complete List of Authors:	Gentry, Brian; University of Pittsburgh, Mechanical Engineering and Materials Science Choi, Tae Hoon; University of Pittsburgh, Chemical & Petroleum Engineering Belfield, William ; Loughborough University Department of Chemical Engineering Keith, John; University of Pittsburgh, Chemical & Petroleum Engineering

SCHOLARONE™  
Manuscripts

Cite this: DOI: 00.0000/xxxxxxxxxx

# Computational predictions of metal-macrocyclic stability constants require accurate treatments of local solvent and pH effects<sup>†</sup>

Brian M. Gentry,<sup>a</sup> Tae Hoon Choi,<sup>a</sup> William S. Belfield,<sup>b</sup> and John A. Keith<sup>\*a</sup>

Received Date

Accepted Date

DOI: 00.0000/xxxxxxxxxx

Rational design of molecular chelating agents requires a detailed understanding of physicochemical ligand-metal interactions in solvent phase. Computational quantum chemistry methods should be able to provide this, but computational reports have shown poor accuracy when determining absolute binding constants for many chelating molecules. To understand why, we compare and benchmark static- and dynamics-based computational procedures for a range of monovalent and divalent cations binding to a conventional cryptand molecule: 2.2.2-cryptand ([2.2.2]). The benchmarking comparison shows that dynamics simulations using standard OPLS-AA classical potentials can reasonably predict binding constants for monovalent cations, but these procedures fail for divalent cations. We also consider computationally efficient static procedure using Kohn-Sham density functional theory (DFT) and cluster-continuum modeling that accounts for local microsolvation and pH effects. This approach accurately predicts binding energies for monovalent and divalent cations with an average error of 3.2 kcal mol<sup>-1</sup> compared to experiment. This static procedure thus should be useful for future molecular screening efforts, and high absolute errors in the literature may be due to inadequate modeling of local solvent and pH effects.

## Introduction

Chelating agents, or chelants, are organic compounds that bind to metal ions in solution, trapping them and limiting their interactions with surrounding environments by forming chelates. A variety of physicochemical interactions determine chelate thermodynamic stability constants, which can vary by several orders of magnitude between different metal ions. Chelants' versatility in selectively binding to specific metal ions gives them a wide range of applications, for example in paper and pulp processing, in detergents to soften water, in medicinal removal of toxic metals from humans, and as nutritional supplements for agricultural crops.<sup>1-5</sup>

Indeed, chelating agents comprise a significant portion of industrial chemical syntheses. In 1999, over 31 200 tons of ethylene diamine (EDA) – a precursor to the common chelating agent ethylene diamine tetraacetic acid (EDTA) – were produced solely for

the synthesis of chelating agents.<sup>6</sup> In 2018, the global agricultural chelant market was valued at \$489.20 million, and it is expected to grow to almost \$1 billion by 2027.<sup>7</sup> However, there is growing concern that existing chelating agents are accumulating in ecosystems due to their high stability and water solubility,<sup>8</sup> a combination of factors that result in higher concentrations of chelants at endpoints in the water cycle. In 2002, Nowack reported that of all organic compounds, EDTA had the highest concentration in river water.<sup>9</sup> Accumulation of chelants can have a detrimental impact on the bioavailability of metal ions, and so chelating agents have been identified as a class of compounds that have large potential for improvement in sustainability.<sup>10</sup> However, there has been limited progress identifying viable alternatives to existing chelants, which are well-entrenched in global economies, since experimental trial and error testing can be time-consuming and expensive.

Thus, there is a growing need to computationally design molecular chelants that bind selectively to assorted metal ions while simultaneously being biodegradable. Computational quantum chemistry can provide accurate knowledge and insight about atomic scale molecular structure/property relationships, and so computational explorations of novel chelants should be productive. Unfortunately, the computational modeling literature has only a few examples of benchmarking studies that focused on the

<sup>a</sup> University of Pittsburgh, Department of Chemical Engineering, 3700 O'Hara Street, Pittsburgh, PA 15261, USA. Fax: +1 412 624 9639; Tel: +1 412 624 7016; E-mail: jakeith@pitt.edu

<sup>b</sup> Loughborough University, Department of Chemical Engineering, Epinal Way, Loughborough, Leicestershire LE11 3TU, UK

<sup>†</sup> Electronic Supplementary Information (ESI) available: [details of any supplementary information available should be included here]. See DOI: 00.0000/00000000.

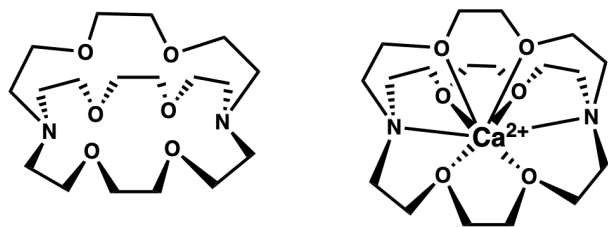


**Fig. 1** Molecular structure of [2.2.2] (left) and  $\text{Ca}^{2+}$  complex with [2.2.2] (right). Metal ions are trapped inside the cage formed by the ether bridges during complexation.

prediction of chelate stability constants. Of those, procedures that use inexpensive continuum solvation models appear to only perform well when calculating *relative* stability constants rather than *absolute* stability constants.<sup>11–13</sup> Agulhon et. al.<sup>14</sup> studied the urinate-bivalent metal ions by using static quantum mechanical calculations with explicit water molecules. However, in those systems the explicit waters do not fully solvate the metal-ligand complex because only two or three water molecules were coordinated to only the metal ions. They also determined *relative* stability trends for divalent cations compared to experiment (rather than directly calculating *absolute* trends). Alternatively, Plazinski carried out classical molecular dynamics to calculate calcium binding by polyguluronate chains using the modified parameterizations of Lennard-Jones 12-6 potentials,<sup>15</sup> while Merz and coworkers have shown that simulating the ‘chelate effect’ with molecular dynamics simulations becomes possible with parameterizations of Lennard-Jones 12-6-4 potentials.<sup>16</sup> In the latter work, the authors caution against the transferability of these parameters to other systems. Thus, there are opportunities for developing *in silico* schemes for absolute stability constant predictions that would better facilitate wider searches of hypothetical chelants. We set out to critically evaluate how different computational approaches perform when predicting absolute chelate binding energies.

### Cryptands and cryptates

Cryptands are macrocyclic chelating agents that trap metal ions inside their cages formed by the branches of the cryptand, coordinating the Lewis base atoms of the chelant (oxygen and nitrogen) with the metal cation to form a cryptate complex. Figure 1 shows the structure of 2.2.2-cryptand ([2.2.2]) encapsulating a calcium cation. Unlike more widely used chelants like nitrilotriacetic acid (NTA) and EDTA that have carboxylic acid groups with torsional degrees of freedom, cryptands are more conformationally constrained, and which we posited would lower the challenge of determining global minima structures to be used in analyses. There are also only a few quantum chemistry studies that have reported cryptate stability constants (*vide infra*), and thus we saw an opportunity for new findings by investigating these systems.

As with chelants in general, the binding affinity of cryptands is known to be controlled by complex combinations of enthalpic and entropic effects. Experimental studies have found that size-matching between the metal ion and cryptand cage plays a vital role, as smaller metal ions can induce steric strain in the cryptand when coordinating with the Lewis base atoms of the cryptand,

reducing the binding interaction.<sup>17</sup> Entropic effects play a vital role as well. Whereas chelate formation normally is understood to bring a significant increase in entropy upon binding (driven by the release of water molecules in the first solvent shell of the solvated ion), cryptate formation does not necessarily result in a noticeable increase in entropy, and can even yield a decrease in entropy with larger, less hydrated cations since the increase in entropy driven by the release of solvent molecules is counteracted by the loss of disorder of the cryptands themselves upon binding.<sup>18,19</sup> Additionally, while some chelants with more torsional freedom such as 2,2',2'',2'''-(*trans*-Cyclohexane-1,2-diylbis(azanetriyl))tetraacetic acid hydrate (CDTA) “preorganize” to facilitate chelation, cryptands do not. Without the presence of a metal ion, the mostly hydrophobic cryptand folds in onto itself, and must first open its cage to allow the entry of a metal ion, lowering the stability constant by a couple orders of magnitude.<sup>20</sup>

As mentioned above, first principles attempts to predict absolute stability constants for chelates (and cryptates) have either been not reported or not successful without empiricism. Wipff and Auffinger used molecular dynamics (MD) simulations with classical forcefields to accurately predict radial distribution functions of the solvent water with cryptates as well as estimates for hydration energies of the ion-[2.2.2] complexes, but they did not explicitly calculate stability constants.<sup>21</sup> Su and Burnette computationally predicted stability constants of [2.2.2] cryptates to metal ions in  $\text{H}_2\text{O}$ , MeOH, and MeCN solvents, and while their modeling captured the qualitative trends in binding energies, they found large systematic errors in absolute binding energies on the order of 20 to 30  $\text{kcal mol}^{-1}$ .<sup>22</sup> Similar attempts to calculate stability constants with other chelating agents have yielded comparable errors. More recently, Gutten and Rulíšek investigated the stability constants of small compounds such as ammonia and acetate with various transition metals, and they found accurate calculate binding constants within 1  $\text{kcal mol}^{-1}$  after correcting for metal-specific and ligand-specific shifts.<sup>13</sup> Although this approach yields highly accurate binding constant predictions, like the parameterized models of Merz and coworkers mentioned above,<sup>16</sup> this approach would be difficult to implement for highthroughput screening studies of broad classes of hypothetical chelants.

With this study we aimed to establish a generalizable calculation scheme for computationally predicting accurate stability constants for [2.2.2] to different metal ions. We hypothesized that previous reported errors in absolute binding constants may have been due to the neglect of modeling local microsolvating environments as well as a need for accounting for pH effects. We tested this hypothesis by comparing three different computational schemes. The first scheme used classical MD simulations with free energy perturbation (FEP) calculations modeling the cryptate in a box of explicit water molecules. The second scheme used standard thermodynamic cycles with energies calculated using static quantum chemistry and a continuum solvation method. The third scheme augmented the second by a) including a microsolvating environment around the metal ion when bound within the cryptand and b) noting that [2.2.2] at pH 7 would be a protonated species. Figure 2 shows an overview of the calculation

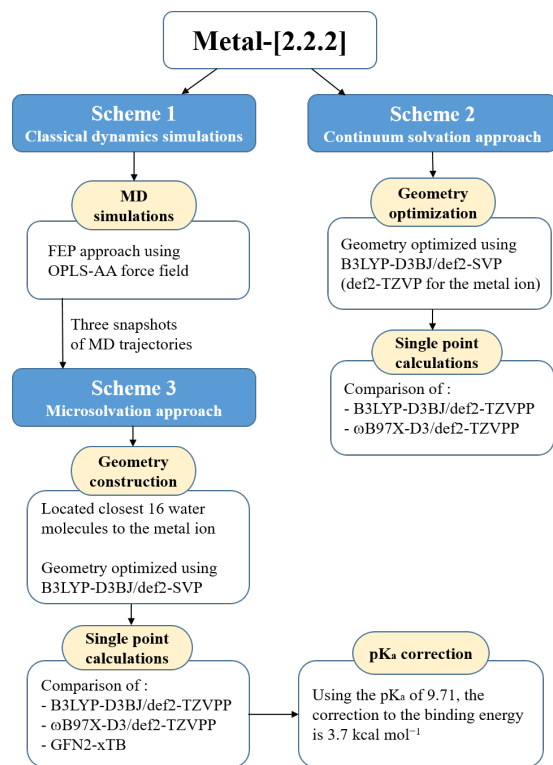


**Fig. 2** Overview of the calculation schemes for predicting the stability constants for Metal-[2.2.2] complexes

schemes for predicting the stability constants for [2.2.2] to different metal ions employed in this study.

## Methods

### Experimental data

Reference experimental stability constants come from ref. 23 for the  $\text{Zn}^{2+}$  complex and from ref. 18 for all other complexes. We note that Arnaud and coworkers reported that  $\text{Zn}^{2+}$  only weakly binds to [2.2.2] with a binding constant less than 2.5, and they stated that their potentiometry approach could not accurately measure small binding constants.  $\text{Zn}^{2+}$  also has a rather small ionic radius, just 74 pm, while the relatively large cavity of [2.2.2] can accommodate much larger ions such as  $\text{K}^+$  (radius = 146 pm) and  $\text{Rb}^+$  (radius = 152 pm). Thus, the experimental value for  $\text{Zn}^{2+}$  is understood to be uncertain. Experimental stability constants were converted to free energy differences using Equation (1), and these are shown in Table 1.

$$\Delta G_{L-M}^{\text{exp}} = -RT \ln K_{L-M} \approx -2.303RT \log_{10} \beta \quad (1)$$

Note that this expression does not account the ionic strength of the solution in which the binding constants were measured, a factor that can change the binding energy by as much as 1 kcal mol<sup>-1</sup>. To obtain a general expression of the binding constant as a function of the ionic strength using Debye-Hückel theory,<sup>24</sup> at least three data points are needed for each ion-[2.2.2] complex. In general, not enough consistent data exists from the reference papers to rigorously extrapolate such values, and so the binding constants are taken as is, noting that there is additional

**Table 1** Experimental [2.2.2] cryptate binding constants, binding energies, corrected ion solvation energies, and respective ionic radii for metal ions.

Ion	$\log_{10}(\beta)$	$\Delta G_{L-M}^{\text{exp a}}$	$\Delta G_s^{\text{exp a,b}}$	Ionic radius (pm) <sup>c</sup>
$\text{H}^+$	9.71	-13.4	—	—
$\text{Na}^+$	4.11	-5.4	-91.1	99
$\text{K}^+$	5.58	-7.7	-74.4	146
$\text{Rb}^+$	4.06	-5.6	-69.6	152
$\text{Ca}^{2+}$	4.57	-6.2	-363.8	100
$\text{Sr}^{2+}$	8.26	-11.4	-333.9	118
$\text{Zn}^{2+}$	$\leq 2.5$	$\geq -3.5$	-471.5	74
$\text{Pb}^{2+}$	12.36	-16.9	-344.7	119

<sup>a</sup> Reported in kcal mol<sup>-1</sup>.

<sup>b</sup> Ionic solvation energies are taken from Ref. 25 and corrected by subtracting 3.8 kcal mol<sup>-1</sup> from each value to account for an error in standard-state corrections correctly provided in Ref. 26.

<sup>c</sup> Ionic radii taken from Ref. 31.

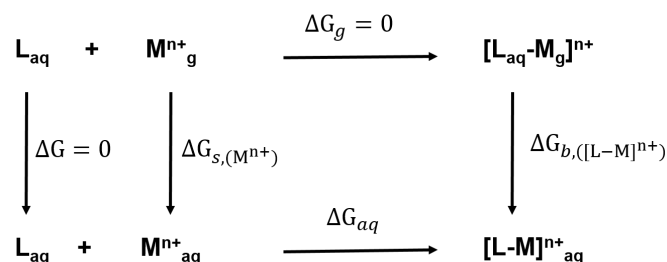


**Fig. 3** Calculation Scheme 1 — MD simulations of solvation and binding energies.

uncertainty of at least 1 kcal mol<sup>-1</sup> on all values as a result of ionic strength variation.

Experimental ion solvation energies were taken from Marcus,<sup>25</sup> but these warrant some minor discussion. First, each reference value is corrected by subtracting 3.8 kcal mol<sup>-1</sup> from each value to account for an error in standard-state corrections correctly provided in Ref. 26. Second, when reporting the ion solvation energies, Marcus makes an extrathermodynamic assumptions as used in the TATB hypothesis. Recent papers have questioned and reached different conclusions about the validity of the TATB hypothesis in aqueous solution.<sup>27,28</sup> Additionally, these experimental solvation energies are measured relative to the solvation energy of a proton, which Marcus treated as having an inherent uncertainty of 1.4 kcal mol<sup>-1</sup>. Since the proton solvation energy plays a central role in establishing relative solvation energies, we assign this uncertainty for all ions, but the actual uncertainties assigned for any ion may in fact be larger based on uncertainties arising from the TATB approximation and other experimental uncertainties. Note that the (corrected) experimental data are generally understood to not include a surface potential contribution, and these also align well with quasi chemical theory calculations by Rempe and co-workers.<sup>29,30</sup>

### Scheme 1: Classical dynamics simulations

Computational Scheme 1 uses aqueous-phase binding free energies determined from the thermodynamic cycle shown in Figure 3. This thermodynamic cycle mirrors the “double-decoupling” method used by Jiao et al. to calculate protein-ligand binding energies.<sup>32</sup>  $\Delta G_{\text{aq}}$  was calculated using Equation (2).

$$\Delta G_{\text{aq}} = \Delta G_{\text{b},([\text{L-M}]^{n+})} - \Delta G_{\text{s},(\text{M}^{n+})} \quad (2)$$

$\Delta G_{\text{s},(\text{M}^{n+})}$  is the solvation energy of the metal ion  $\text{M}^{n+}$  calculated from a free-energy perturbation (FEP) approach in which the electrostatic and van der Waals interactions are slowly scaled from 0 to 1 (i.e. a technique referred to as ‘computational alchemy’).<sup>33</sup>  $\Delta G_{\text{b},([\text{L-M}]^{n+})}$  is obtained by tuning out electrostatic and van der Waals interactions between the metal ion and both the [2.2.2] and solvent water while keeping the metal ion inside the [2.2.2] cage.

All MD simulations were carried out using TINKER 8.6.<sup>34</sup> We assigned atom types for [2.2.2] using the OPLS all-atom force field (OPLS-AA).<sup>35</sup> Partial charges for [2.2.2] were taken from previous work,<sup>21</sup> which were obtained using an *ab initio* method with the 6-31G\* basis set, and an electrostatic potential-based fitting method (see the ESI<sup>†</sup> for the partial charges). While we could derive our own partial charges, those derived by Auffinger and Wipff yielded reasonable hydration dynamics, and so we opt to use them to calculate binding energies. Standard parameters for Coulombic and van der Waals interactions for alkali metals, alkaline earth metals, and  $\text{Zn}^{2+}$  were taken from the OPLS force field. No parameters exist for  $\text{Pb}^{2+}$  (or for most transition/post-transition metals) in the OPLS force field, which poses a limitation on an MD-based approach for determining stability constants with metals outside the s-block. For each case, the metal ion was placed in the center of the [2.2.2] cage, and the resulting cryptate was placed in a box of TIP3P water with side lengths 30 Å. The box was minimized until the RMS gradient per atom reached 1.0 kcal/(mol·Å). The FEP approach uses Equation (3) to calculate energies and forces at each dynamical step, where the electrostatic and van der Waals interactions between the metal ion and surrounding environment are incrementally tuned out by running numerous MD simulations at different  $\lambda$  values (see SI for  $\lambda$  steps).

$$E_{\text{total}} = E_{\text{bonded}} + \lambda_{\text{elec}} E_{\text{elec}} + \lambda_{\text{vdw}} E_{\text{vdw}} \quad (3)$$

All MD simulations were carried out using periodic boundary conditions; Ewald summation for long-range electrostatic interactions; the Berendsen thermostat and barostat to control temperature and pressure, respectively; and the Verlet algorithm to integrate velocity steps. In each simulation, the box containing the cryptate complex was equilibrated for 100 ps under the NPT ensemble and then 250 ps under the NVT ensemble. A subsequent 250 ps of production runs were carried out under the NVT ensemble, where frames were saved every 2 ps. A time step of 2 fs was used for all MD simulations. The Bennett acceptance ratio (BAR) method was used to reconstruct changes in free energy from the MD simulations.<sup>36</sup>

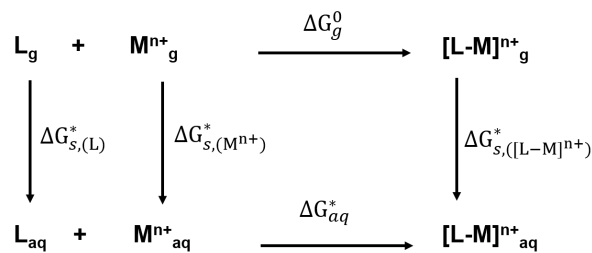


**Fig. 4** Calculation Scheme 2 — Implicit solvation treatment of neutral ligand, implicit solvation treatment of charged species.

### Scheme 2: Continuum solvation approach

In Scheme 2, aqueous-phase binding free energies were calculated with electronic structure calculations using the thermodynamic cycles shown in Figure 4. The solvation energy of [2.2.2] and the ion-[2.2.2] complexes are treated using a continuum solvation model (the conductor-like polarizable continuum model, CPCM),<sup>37–40</sup> while experimental solvation energies from Marcus<sup>25</sup> are used for the single ions.

Following Ben-Naim and Marcus,<sup>26,41</sup> each  $\Delta G_{\text{s}}^*$  was calculated according to Equation (4),

$$\Delta G_{\text{s}}^* = (G_{\text{aq}} - G_{\text{g}}) + \Delta G_{\text{s}}^{\circ \rightarrow * *} \quad (4)$$

where  $G_{\text{g}}$  and  $G_{\text{aq}}$  denote the gas-phase and aqueous-phase free energies, respectively (their difference yielding the work to transfer a solute into solvent at a standard state of 1M), and  $\Delta G_{\text{s}}^{\circ \rightarrow *}$  is a correction associated with transferring a molecule from a gas-phase standard state to aqueous-phase standard state; this correction equals 1.89 kcal mol<sup>-1</sup> at 298 K.<sup>42</sup> where the superscript  $\circ$  and  $*$  denote the gas and liquid standard state of 1 atm and 1 M, respectively. The gas-phase free energy  $G_{\text{g}}$  was calculated for each species by  $G_{\text{g}} = E_{\text{g}} + \delta g$ , where  $E_{\text{g}}$  is the gas-phase electronic energy and  $\delta g$  is a correction term that includes the zero-point vibrational energy, enthalpic terms, and entropic terms from the standard ideal gas, rigid rotor, and harmonic oscillator approximations. Summing all terms, the aqueous-phase binding energy is given by Equation (5).

$$\begin{aligned} \Delta G_{\text{aq}}^* = & E_{\text{aq},([\text{L-M}]^{n+})} + \delta g_{[\text{L-M}]^{n+}} - E_{\text{aq},(\text{L})} - \delta g_{\text{L}} \\ & - E_{\text{g},(\text{M}^{n+})} - \delta g_{\text{M}^{n+}} - \Delta G_{\text{s},(\text{M}^{n+})}^{\text{exp}} - \Delta G_{\text{s}}^{\circ \rightarrow * *} \end{aligned} \quad (5)$$

For both the uncomplexed [2.2.2] and the metal-[2.2.2] complexes without explicit waters, the initial structures were generated using Avogadro.<sup>43</sup> The uncomplexed [2.2.2] structure was optimized with the B3LYP-D3BJ<sup>44–47</sup>/def2-SVP<sup>48,49</sup> model chemistry. The metal-[2.2.2] complexes used the same method, but with the def2-TZVP basis set for the metal ion, which involves an effective core potential for rubidium, strontium, and lead cases (see the ESI<sup>†</sup> for the optimized geometries). Frequency calculations after the geometry optimizations confirmed that all structures were at a local minimum. Single-point energy calculations were carried out for both the gas-phase energy and aqueous-phase energy using B3LYP-D3BJ and  $\omega$ B97X-D3<sup>50</sup> with the def2-

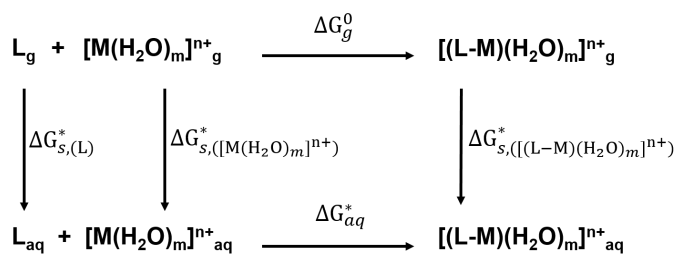


**Fig. 5** Calculation Scheme 3 — Implicit solvation treatment of neutral ligand, mixed implicit/explicit solvation treatment of charged species.

TZVPP basis sets. All DFT calculations used the RIJCOSX approximation as implemented in ORCA.<sup>51</sup>

### Scheme 3: Microsolvation approach

In Scheme 3, the solvation of [2.2.2] is again treated using the implicit CPCM model, but the charged species (both the complex and the single ion) are treated with a microsolvation approach, where the molecules are surrounded by  $m$  water molecules to capture local solvent effects. The convergence of geometries and energies of ion-water clusters were previously studied by our group<sup>52</sup> by increasing  $m$ , and the clusters are well-converged for these cases by  $m = 16$ . Figure 5 shows the thermodynamic cycle for Scheme 3. The resulting binding energy is calculated in Equation (6). While additional corrections are usually needed to account for the standard state water molecules in liquid water (55.34 M) in Scheme 3, the construction of this thermodynamic cycle cancels the contributions out, and so they are omitted in subsequent analysis.

$$\begin{aligned}
 \Delta G_{aq}^* = & E_{aq,([(L-M)(H_2O)_m]^{n+})} + \delta g_{[(L-M)(H_2O)_m]^{n+}} - E_{aq,(L)} - \delta g_L \\
 & - E_{aq,([M(H_2O)_m]^{n+})} - \delta g_{M(H_2O)^{n+}} - \Delta G_s^{\circ \rightarrow *}
 \end{aligned} \quad (6)$$

For the conformational explorations, a QM/MM method can provide accurate sampling of metal-ligand conformers, but these would be too computationally demanding for anticipated high-throughput screening studies. Instead, we followed a similar procedure that was previously used in Ref.<sup>53</sup> for small ions. Here, three snapshots of MD trajectories were taken from the earlier MD simulations when available for the ions, and the closest 16 waters to the metal ion were carved out. Again, we could not find suitable OPLS-AA parameters for  $Pb^{2+}$  that allowed dynamics simulations for this metal, so we used microsolvated structures from the  $Sr^{2+}$  simulations since  $Pb^{2+}$  and  $Sr^{2+}$  have the same charge and very similar ionic radii. Note that the conformers we obtain from classical MD simulations serve as merely a starting point to find the optimal microsolvated structures from subsequent DFT optimizations. All microsolvated structures then underwent a B3LYP-D3BJ/def2-SVP geometry optimization (see the ESI<sup>†</sup> for the optimized geometries). Boltzmann averages of the resulting aqueous free energies (three structures for each cryptate) were taken to represent an approximate ensemble average for the

clusters, accounting for minor changes in conformational differences and solvent arrangements.

Previous analyses of the binding of [2.2.2]<sup>22</sup> have modeled the scenario where an unprotonated [2.2.2] molecule binds with a metal ion. However, the reported  $pK_a$  of [2.2.2] is between 9.7<sup>18</sup> and 10.0<sup>23</sup>, indicating that [2.2.2] will be protonated in a roughly 1000:1 ratio at neutral pH. Hence, there is a need to make an analytical correction due to deprotonation of [2.2.2] prior to complexation. The analytical correction is given by Equation (7)<sup>54</sup>, where  $\Delta G_{aq}^{corr}$  is the observed free energy,  $pK_a^{(L-M)}$  is the  $pK_a$  of the ion-[2.2.2] complex, and  $pK_a^{(L)}$  is the  $pK_a$  of [2.2.2].

$$\Delta G_{aq}^{corr} = \Delta G_{aq} - k_b T \ln \left( \frac{1 + 10^{pK_a^{(L-M)} - pH}}{1 + 10^{pK_a^{(L)} - pH}} \right) \quad (7)$$

While a full analysis of the pH-dependence of the binding energy would require  $pK_a$  calculations of all ion-[2.2.2] complexes, the proximity of a metal ion and a positively charged proton within the cage of such a protonated species is likely to produce a highly unfavorable interaction, suggesting that the  $pK_a$  shift during complexation will be large and negative. Therefore,  $pK_a^{(L-M)} - pH$  will be very negative and the numerator in the logarithm can be approximated as 1. An approximation to the change in energy is given by Equation (8).

$$\Delta G_{aq}^{corr} = \Delta G_{aq} - k_b T \ln \left( \frac{1}{1 + 10^{pK_a^{(L)} - pH}} \right) \quad (8)$$

Using the literature  $pK_a$  of 9.71<sup>18</sup>, the correction to the binding energy at neutral pH is 3.7 kcal mol<sup>-1</sup>.

We also benchmarked the energies of the cryptates in Scheme 3 using the recently published and highly promising GFN2-xTB method,<sup>55</sup>. This semiempirical method is highly efficient and in principle can be applied to the cryptates in computational screening approaches without any parameterization. Our optimized structures from B3LYP calculations were re-optimized using GFN2-xTB, and aqueous-phase single-point energy calculations were carried out with the generalized born-based implicit solvation model (GBSA)<sup>56</sup> that is implemented in the standalone xTB program.<sup>55</sup> Hessian calculations provided the thermodynamic correction term and confirmed the structures were at a local minimum.

## Results

### Local solvation analysis

Continuum solvation models generally do not account for long-range electrostatic interactions which significantly affect energetics of charged species<sup>57,58</sup>. Thus, these models can bring errors when the solvated system has a concentrated partial charge near the CPCM cavity boundary or a large polarity difference within the molecule. Now-conventional wisdom about continuum solvent models suggests that solvation energies from these methods will be less accurate with charged species. Local solvation structure is likely a contributing factor in cryptates, so we investigated the sensitivity of binding energies due to the local geometry of the gas-phase optimized chelates with and without explicit

**Table 2** Coordination numbers of each ion analyzed with MD in solution and within [2.2.2].

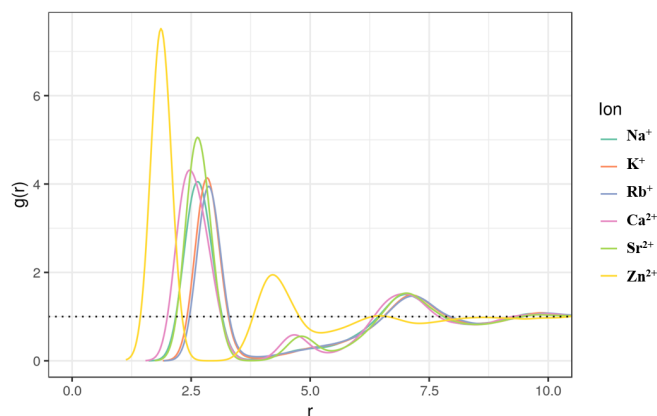
Ion	$n_{Ow}$	$n_{Ow}$ in [2.2.2] cage	$n$ in [2.2.2] cage	$r'$ (Å)
Na <sup>+</sup>	6.2	0.9	9.0	2.6
K <sup>+</sup>	7.4	1.2	9.3	2.9
Rb <sup>+</sup>	8.2	0.9	9.0	2.9
Ca <sup>2+</sup>	8.0	2.0	10.0	2.5
Sr <sup>2+</sup>	8.3	2.0	10.0	2.6
Zn <sup>2+</sup>	6.1	6.1	6.1	1.9

water molecules. Radial distribution functions (RDFs) of water molecules were generated from the classical MD simulations to determine how local water molecules interact with the ion while it is bound inside the [2.2.2] molecule.

The RDF of each cation relative to the oxygen and nitrogen atoms in [2.2.2] and surrounding water solvent are shown in Figure 6. The RDF for the alkali and alkaline earth metal cations show a first coordination sphere from 2.5 to 2.9 Å, while the first coordination sphere for Zn<sup>2+</sup> is much closer at 1.9 Å. These RDFs agree well with those obtained by Wipff and Auffinger<sup>21</sup>. Coordination numbers were then calculated based on Equation (9), where  $r'$  represents the location of the first minimum of the RDF and  $\rho$  is the density of the bulk solvent (here, 0.0334 molecules/Å<sup>3</sup> for water).

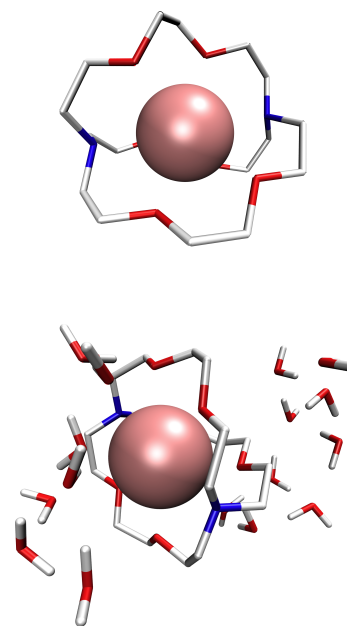
$$n = 4\pi\rho \int_0^{r'} r^2 g(r) dr \quad (9)$$

Coordination numbers for various ions are shown in Table 2. “ $n_{Ow}$ ” is the average coordination number of the cation in solvent water, while “ $n_{Ow}$  in [2.2.2] cage” represents the coordination number to the metal ion while the ion is inside the cage. Finally, “ $n$  in [2.2.2] cage” is the coordination number of the cation to any Lewis base, which includes the amine and ether groups on [2.2.2] as well as solvent water. For the monovalent cations, the ion is coordinated to all eight Lewis base atoms in [2.2.2] as well

**Fig. 6** Radial distribution functions (RDFs) for ions to coordinating oxygen and nitrogen atoms from [2.2.2] and oxygens from surrounding water solvent.**Table 3** Distances between the ion and the center-of-mass (CM) for [2.2.2] ( $r$ ) in DFT-optimized geometries without explicit solvent (*in vacuo*) and with explicit solvent.

Ion	$r$ in <i>vacuo</i> (Å)	$r$ in solvent (Å)
Na <sup>+</sup>	0.160	0.457 ± 0.088
K <sup>+</sup>	0.135	0.658 ± 0.064
Rb <sup>+</sup>	0.128	0.424 ± 0.054
Ca <sup>2+</sup>	0.066	0.350 ± 0.056
Sr <sup>2+</sup>	0.073	0.341 ± 0.029
Zn <sup>2+</sup>	0.313	3.638 ± 1.065
Pb <sup>2+</sup>	0.096	0.333 ± 0.065

as one additional water molecule, giving coordination numbers  $n$  of 9.0 for Na<sup>+</sup> and Rb<sup>+</sup> and 9.3 for K<sup>+</sup>. With the alkaline earth metals, the ion coordinated to all Lewis base atoms in [2.2.2] and two additional water molecules, giving  $n = 10.0$  for both ions analyzed. Zn<sup>2+</sup> showed a tendency to exit the [2.2.2] cage and instead be coordinated by solvent water molecules, as evidenced by the constant  $n_{Ow}$  in Table 2. This suggests that interactions between Zn<sup>2+</sup> and [2.2.2] in solution may not even be strong enough for chelation to occur, which is still consistent with the qualitative binding constant reported by Arnaud.<sup>23</sup>

**Fig. 7** [2.2.2] complexes with K<sup>+</sup>, with and without explicit water molecules.

We also report the average ion-center of mass distance in DFT-optimized geometries to illustrate the importance solvent water molecules play. Table 3 summarizes the distances between the ions and the center of mass of [2.2.2]. In particular, we note that for every metal ion, the average distance between the ion and the center-of-mass (CM) for [2.2.2] increases significantly from *in vacuo* to solvent by at least 0.25 Å. This increase in distance

comes as a result of the [2.2.2] cage “opening up” to allow water molecules to coordinate with the ion, adopting a tent-like configuration as shown in Figure 7, where two cryptand branches lie in the same plane and the third acts as the spine of the “tent”. Furthermore, the average distance between  $\text{Zn}^{2+}$  and the CM for [2.2.2] was very large at 3.638 Å as shown in Figure 8. This occurred because after DFT-optimization,  $\text{Zn}^{2+}$  left the cage and became mostly solvated by water molecules, relieving some of the steric strain associated with placing the ion inside the cage. This again supports the hypothesis that the interactions between  $\text{Zn}^{2+}$  and [2.2.2] are too weak to promote chelation.

We emphasize that the large difference in gas-phase optimized geometries with and without explicit waters reveals a two-fold importance for using a mixed implicit/explicit solvation scheme. First, including explicit water molecules shields the positive charge within the cage from the CPCM cavity thus yielding more accurate solvation energies. Second, explicit water molecular interactions stabilize the otherwise strained [2.2.2] molecule in the absence of solvent molecules.

### Binding energies

The resulting binding energies for all schemes are shown in Table 4. Scheme 1 accurately reproduced the binding energy of cryptates of monovalent cations with an MAE of  $1.7 \pm 0.8 \text{ kcal mol}^{-1}$ . The model overbound  $\text{Na}^+$  and  $\text{K}^+$  by about  $2 \text{ kcal mol}^{-1}$  each, while it underbound  $\text{Rb}^+$  by  $1.0 \text{ kcal mol}^{-1}$ . These magnitudes in errors are relatively small and were not considered concerning. However, energies were significantly higher for divalent cations, and positive rather than negative binding energies were predicted using this Scheme 1 (giving an MAE for

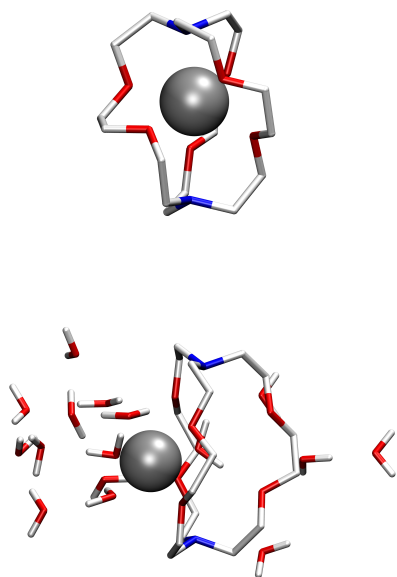


**Fig. 8** [2.2.2] complexes with  $\text{Zn}^{2+}$ , with and without explicit water molecules.

the divalent cations of  $31.8 \text{ kcal mol}^{-1}$ , and a maximum error of  $35.9 \text{ kcal mol}^{-1}$  for  $\text{Ca}^{2+}$ ). For reference, the overall MAE for Scheme 1 was  $16.7 \text{ kcal/mol}$ . We note that there are numerous strategies to incorporate assorted metal ions into force fields, including reparameterizations of the electrostatic and van der Waals potentials as well as development of polarizable parameters, such as those in the AMOEBA force field,<sup>59</sup> for the ligand and metal interactions, but parameterization schemes for these approaches would likely not be easily transferable for rapid screening.

Highly transferable schemes such as Scheme 2 are appealing, but this approach was found to perform even worse than Scheme 1. The implicit solvation scheme drastically overbound the metal ions to [2.2.2], predicting binding energies that were significantly more negative than experimental values. These errors are in line with those from Su and Burnette’s results,<sup>22</sup> where they used a 4 cluster model,  $\text{M}^+(\text{solv})_4$ . The significant deviations from experimental values suggests that blindly applying a continuum solvation model in this situation will yield erroneous results; as we explained in the previous section, local solvent effects play an important role in both the actual calculation of the solvation energies and in the global minimum structures.

When we account for local solvent effects using a microsolvation approach, the binding energies improve drastically. The binding energies in Scheme 3 are shown in Table 4, where the MAE with the B3LYP-D3BJ functional is  $6.4 \pm 4.2 \text{ kcal mol}^{-1}$  and  $4.8 \pm 3.1 \text{ kcal mol}^{-1}$  with the  $\omega\text{B97X-D3}$  functional. Interestingly, GFN2-xTB performs well with monovalent cations but has much larger errors for divalent cations, displaying a similar performance as classical force field simulations.

Furthermore, by applying the  $\text{pK}_a$  correction, the energies show remarkable agreement to the experimental binding energies for nearly all cases, which are also included with the parentheses Table 4. The energies show remarkable agreement to the experimental binding energies for nearly all cases. The MAE with B3LYP-D3BJ is  $4.2 \pm 2.8 \text{ kcal mol}^{-1}$ , and with  $\omega\text{B97X-D3}$  is  $3.2 \pm 1.5 \text{ kcal mol}^{-1}$ . The largest error with  $\omega\text{B97X-D3}$  resulted from  $\text{Ca}^{2+}$  and  $\text{Zn}^{2+}$ , where the model predicted a binding energy of  $-11.0 \text{ kcal mol}^{-1}$  compared to the experimental value of  $-6.2 \text{ kcal mol}^{-1}$  and  $1.5 \text{ kcal mol}^{-1}$  compared to  $-3.5 \text{ kcal mol}^{-1}$ , respectively. However, due to zinc’s weak binding and the uncertainty in the actual experimental value, we omit this data point from the MAE calculation, which lowers the MAE for B3LYP-D3BJ to  $4.1 \pm 3.1 \text{ kcal mol}^{-1}$  and for  $\omega\text{B97X-D3}$  to  $3.0 \pm 1.5 \text{ kcal mol}^{-1}$ .

For comparison of Scheme 2 and 3, the regression plots between the calculated and experimental binding energies for nine different metal-[2,2,2] complexes are shown in Figure 9. The correlation coefficient ( $R^2$ ) of Scheme 3 are significantly improved from those of Scheme 2 (from 0.26 and 0.37 to 0.84 and 0.86 for  $\omega\text{B97X-D3}$  and B3LYP-D3BJ, respectively).

In the case of GFN2-xTB potential, the binding energies of  $\text{K}^+$  and  $\text{Na}^+$  are very close to the experimental observations. Although those of the divalent cations show significant discrepancy with experimental results, this method still provides a very efficient performance considering the computational cost. Overall,



**Table 4** Calculated binding energies from Scheme 1, Scheme 2, and Scheme 3. (unit: kcal/mol)

Ion	Scheme 1 <sup>a</sup>	Scheme 2 <sup>b</sup>		Scheme 3			Experimental
		B3LYP-D3BJ	$\omega$ B97X-D3	B3LYP-D3BJ	$\omega$ B97X-D3	GFN2-xTB	
Na <sup>+</sup>	-7.9	-44.5	-30.2	-7.5 (-3.8) <sup>c</sup>	-9.8 (-6.1)	-9.3 (-5.6)	-5.4
K <sup>+</sup>	-9.3	-39.9	-26.7	-14.9 (-11.2)	-13.9 (-10.2)	-10.9 (-7.2)	-7.7
Rb <sup>+</sup>	-4.6	-31.8	-20.5	-9.4 (-5.7)	-5.5 (-1.8)	-5.3 (-1.6)	-5.6
Ca <sup>2+</sup>	29.7	-50.4	-35.3	-17.2 (-13.5)	-14.7 (-11.0)	6.1 (9.8)	-6.2
Sr <sup>2+</sup>	15.8	-48.5	-35.9	-19.1 (-15.4)	-17.2 (-13.5)	0.7 (4.4)	-11.4
Zn <sup>2+</sup>	28.7	-37.0	-24.8	-2.4 (1.3)	-2.2 (1.5)	8.4 (12.1)	$\geq -3.5$
Pb <sup>2+</sup>		-49.9	-32.4	-28.5 (-24.8)	-24.4 (-20.7)	7.1 (10.8)	-16.9
MAE	16.7	35.0	21.3	6.4 (4.2)	4.8 (3.2)	9.7 (11.4)	

<sup>a</sup> Data for Pb<sup>2+</sup> are omitted here because these parameters do not exist in the OPLS-AA force field.

<sup>b</sup> All binding energies in Scheme 2 have an uncertainty of at least 1.4 kcal mol<sup>-1</sup> due to the uncertainty in the proton solvation energy used to derive these values (see main text for discussion).

<sup>c</sup> Data in the parentheses represent pK<sub>a</sub>-corrected binding energies.

the binding energies calculated with static GFN2-xTB calculation with a microsolvation approach are advantageous over those from the classical MD simulations. Thus, it could be very useful tool for the rapid pre-screening process for several thousands of chelating molecules. Also, the GFN2-xTB scheme can be applicable for the dynamics simulations combined with the enhanced sampling technique<sup>60,61</sup> to generate the free energy profile.

## Conclusions

We have reported progress toward understanding in how to best model physicochemical interactions that influence chelate binding. This study focused on cryptates based on [2.2.2] binding to a variety of monovalent and divalent cations. Previously reported studies have not shown accurate calculations of these values without substantial model parameterization. We tested and benchmarked different computational schemes. Schemes using classical forcefields provided good accuracy for cryptates of monovalent cations, but results were poor for cryptates of divalent cations, and we attribute this to these forcefields inadequately accounting for charge polarization.<sup>62</sup> Semiempirical and DFT-based schemes using static calculations without explicit microsolvation were also insufficiently accurate for most cations. When accounting for pK<sub>a</sub>s, absolute binding energies were finally found to be reasonably accurate.

Calculations using Scheme 3 predict experimental values to 3.2 kcal mol<sup>-1</sup>, which is a significant improvement compared to other schemes used in previous studies. We attribute the accuracy of this scheme to the importance of modeling a local environment of the cryptate as well as accounting for the ligand's actual protonation state at ambient pH. In this case, we used 16 explicit solvent molecules obtained from prior work or MD sampling with generic classical force fields. Thus, we have shown a computational scheme for predicting binding energies that match well with experimental values without requiring *a priori* knowledge. While we select only three snapshots from MD simulations for further DFT calculations, more snapshots may improve the accuracy of this method for different systems, particularly those with high degrees of conformational freedom. For general applications, we

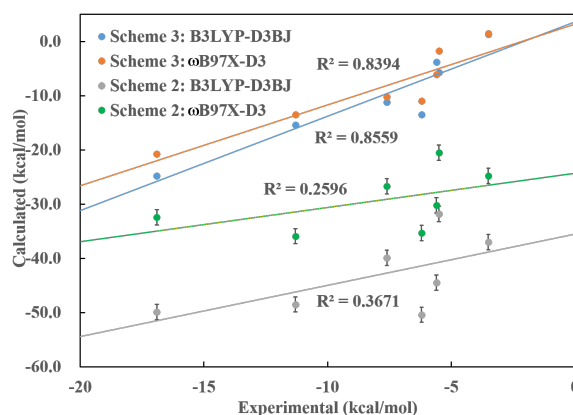


**Fig. 9** Comparison of the experimental and calculated binding energies from Scheme 2 and Scheme 3. See main text for discussion of error bars.

recommend brief MD simulations using generic parameters for the metal ions to obtain a local solvation structure<sup>53</sup> followed by static semiempirical (for monovalent cations) or more accurate DFT calculations (needed for divalent cations).

## Author Contributions

B.M.G. contributed in data curation, formal analysis, investigation, methodology, visualization, and writing - original draft and review & editing. T.H.C. contributed in supervision, validation, visualization, and writing - review & editing. W.S.B. contributed in formal analysis, investigation, methodology, and writing - original draft. J.A.K. contributed in conceptualization, funding acquisition, methodology, project administration, resources, supervision, writing - original draft, and writing - review & editing.

## Acknowledgments

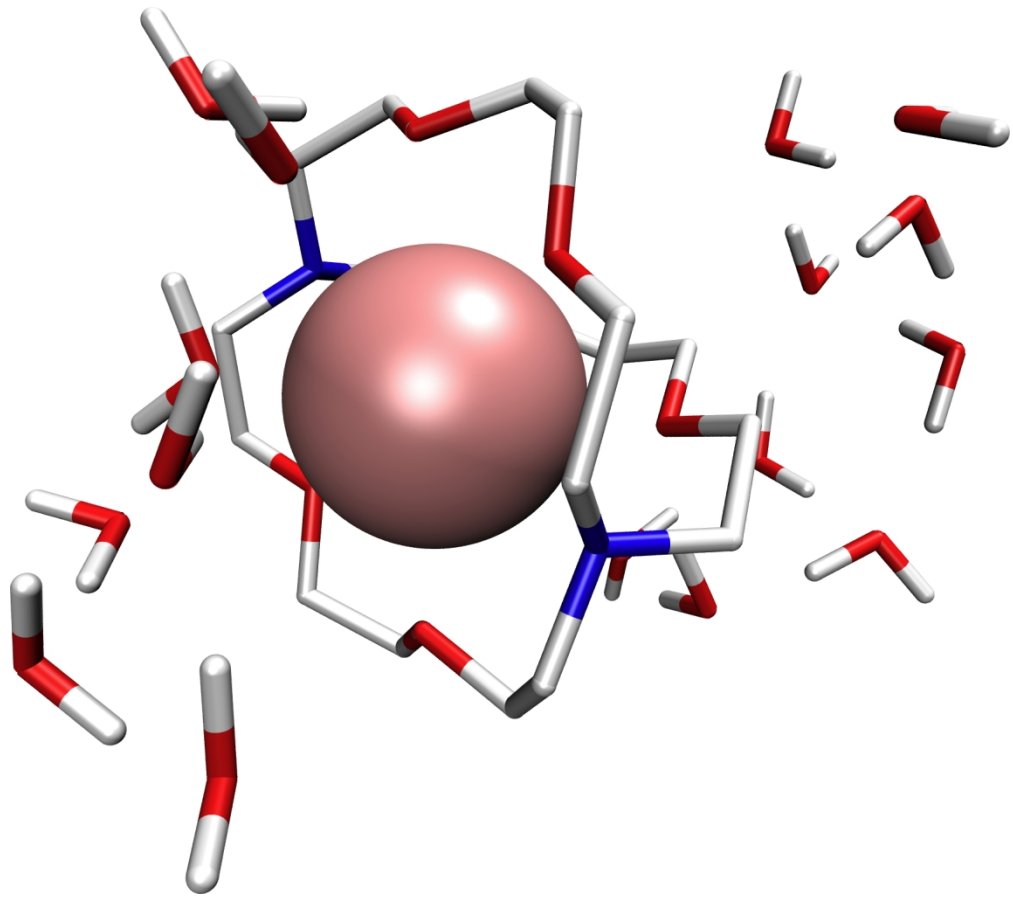
The authors would like to thank the Center for Research Computing at the University of Pittsburgh for computational resources

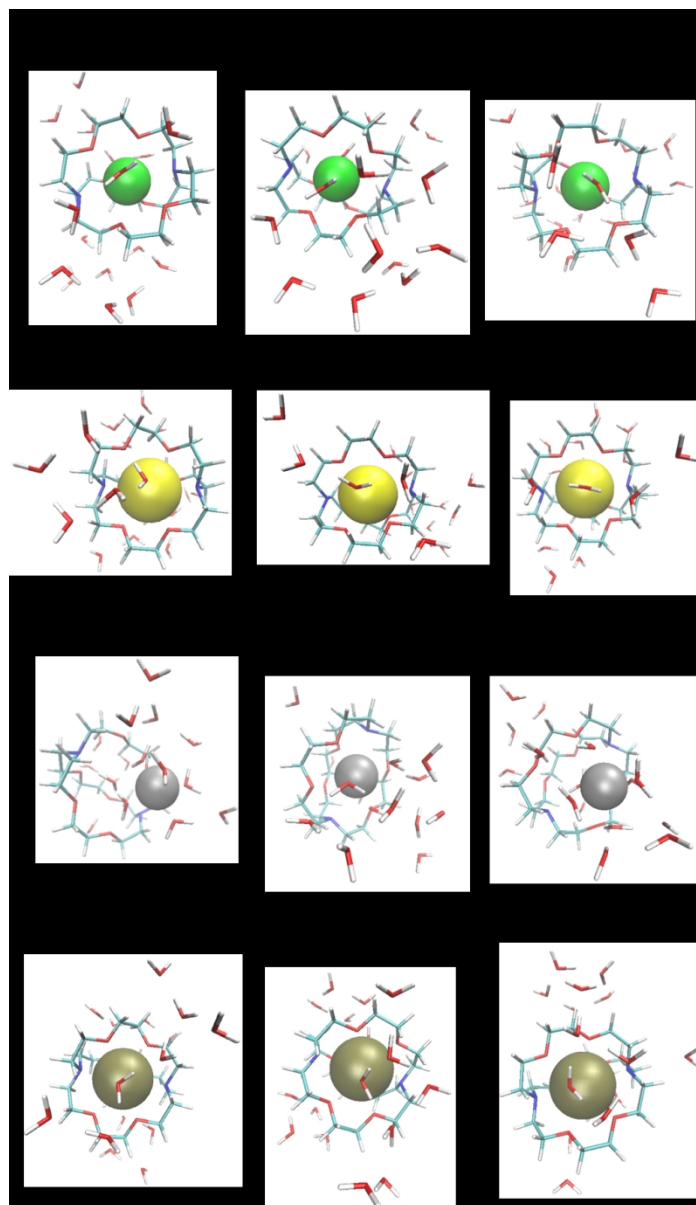
and technical support. This work has been funded by the U.S. National Science Foundation (NSF-CBET 1705592). Acknowledgements are also made to Loughborough University's Department of Chemical Engineering, the University of Pittsburgh's Swanson School of Engineering, and the University of Pittsburgh's Office of the Provost for their financial contributions enabling the completion of this project.

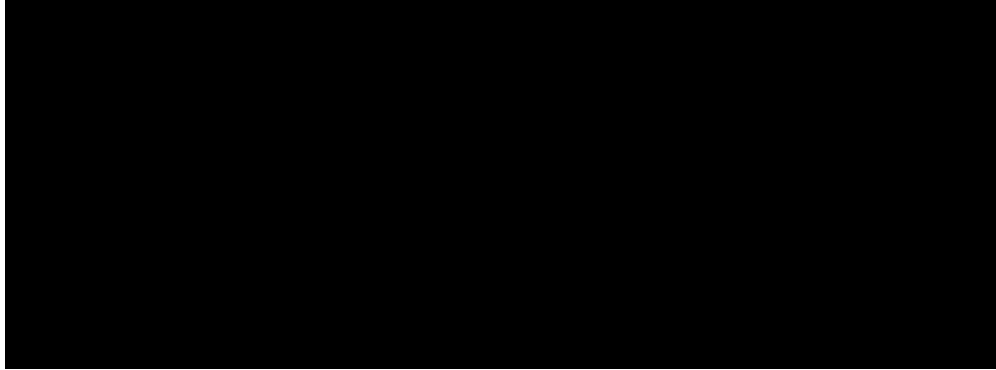
## References

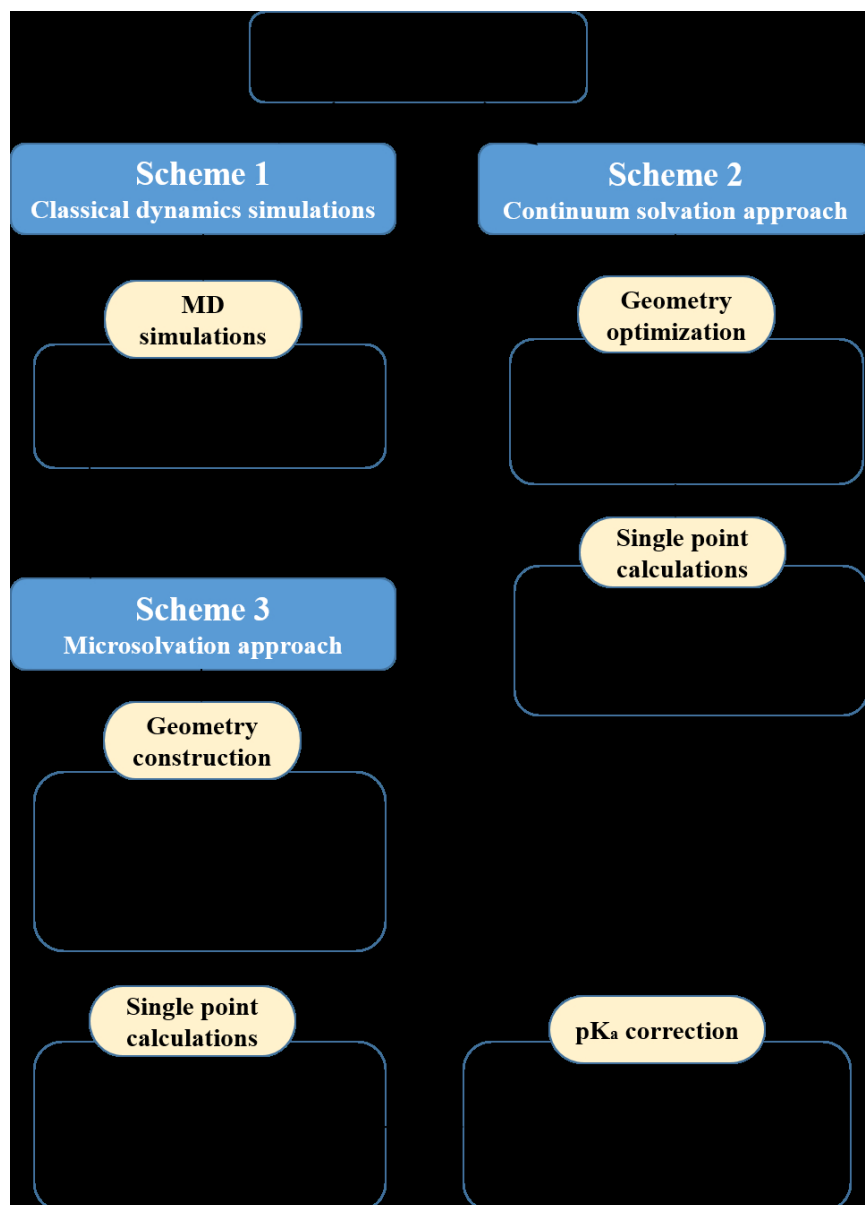
- 1 I. S. Pinto, O. S. Ascenso, M. T. Barros and H. M. Soares, *Int. J. Environ. Sci. Technol.*, 2015, **12**, 975–982.
- 2 A. C. Kogawa, B. G. Cernic, L. G. D. do Couto and H. R. N. Salgado, *Saudi Pharm. J.*, 2017, **25**, 934–938.
- 3 *Br. Med. J.*, 1971, **2**, 270–272.
- 4 A. Kattamis, V. Ladis, H. Berdousi, N. L. Kelekis, E. Alexopoulou, I. Papisotiriou, K. Drakaki, I. Kaloumenou, A. Galani and C. Kattamis, *Blood Cells Mol. Dis.*, 2006, **36**, 21–25.
- 5 B. S. Sekhon, *Resonance*, 2003, **8**, 46–53.
- 6 G. R. Maxwell, *Handbook of Industrial Chemistry and Biotechnology*, Springer US, Boston, MA, 2012, pp. 875–937.
- 7 *Growth Assessment of Worldwide Agricultural Chelates Markets*, 2020.
- 8 C. Oviedo and J. Rodríguez, *Quim. Nova*, 2003, **26**, 901–905.
- 9 B. Nowack, *Environ. Sci. Technol.*, 2002, **36**, 4009–4016.
- 10 P. G. Jessop, F. Ahmadpour, M. A. Buczynski, T. J. Burns, N. B. Green, R. Korwin, D. Long, S. K. Massad, J. B. Manley, N. Omidbakhsh, R. Pearl, S. Pereira, R. A. Predale, P. G. Sliva, H. Vanderbilt, S. Weller and M. H. Wolf, *Green Chem.*, 2015, **17**, 2664–2678.
- 11 M. N. Vo, V. S. Bryantsev, J. K. Johnson and J. A. Keith, *Int. J. Quantum Chem.*, 2018, **118**, year.
- 12 L. Chen, T. Liu and C. Ma, *J. Phys. Chem. A*, 2010, **114**, 443–454.
- 13 O. Gutten and L. Rulišek, *Inorg. Chem.*, 2013, **52**, 10347–10355.
- 14 P. Agulhon, V. Markova, M. Robitzer, F. Quignard and T. Mineva, *Biomacromolecules*, 2012, **13**, 1899–1907.
- 15 W. Plazinski, *J. Comp. Chem.*, 2011, **32**, 2988–2995.
- 16 A. Sengupta, A. Seitz and K. M. Merz, *J. Am. Chem. Soc.*, 2018, **140**, 15166–15169.
- 17 R. D. Hancock and A. E. Martell, *Chem. Rev.*, 1989, **89**, 1875–1914.
- 18 G. Anderegg, *Helv. Chim. Acta*, 1975, **58**, 1218–1225.
- 19 J. M. Lehn, *Acc. Chem. Res.*, 1978, **11**, 49–57.
- 20 A. E. Martell and R. D. Hancock, 2009, 240–254.
- 21 G. Wipff and P. Auffinger, *J. Am. Chem. Soc.*, 1991, **113**, 5976–5988.
- 22 J. W. Su and R. R. Burnette, *ChemPhysChem*, 2008, **9**, 1989–1996.
- 23 F. Arnaud-Neu, B. Spiess and M.-J. Schwing-Weill, *Helv. Chim. Acta*, 1977, **60**, 2633–2643.
- 24 P. W. Debye and E. Huckel, *Phys. Z.*, 1923, **24**, 185.
- 25 Y. Marcus, *J. Chem. Soc., Faraday Trans.*, 1991, **87**, 2995–2999.
- 26 A. Ben-Naim and Y. Marcus, *J. Chem. Phys.*, 1984, **81**, 2016–2027.
- 27 T. P. Pollard and T. L. Beck, *J. Chem. Phys.*, 2018, **148**, 222830.
- 28 T. T. Duignan, M. D. Baer and C. J. Mundy, *J. Chem. Phys.*, 2018, **148**, 222819.
- 29 K. Leung, S. B. Rempe and O. A. Von Lilienfeld, *J. Chem. Phys.*, 2009, **130**, year.
- 30 M. I. Chaudhari, J. M. Vanegas, L. R. Pratt, A. Muralidharan and S. B. Rempe, *Hydration mimicry by membrane ion channels*, 2020, <https://pubmed.ncbi.nlm.nih.gov/32155383/>.
- 31 R. D. Shannon, *Acta Crystallogr.*, 1976, 751.
- 32 D. Jiao, P. A. Golubkov, T. A. Darden and P. Ren, *Proc. Natl. Acad. Sci. U.S.A.*, 2008, **105**, 6290–6295.
- 33 T. P. Straatsma and J. A. McCammon, *Annu. Rev. Phys. Chem.*, 1992, **43**, 407–435.
- 34 J. A. Rackers, Z. Wang, C. Lu, M. L. Laury, L. Lagardère, M. J. Schnieders, J. P. Piquemal, P. Ren and J. W. Ponder, *J. Chem. Theory Comput.*, 2018, **14**, 5273–5289.
- 35 W. L. Jorgensen, D. S. Maxwell and J. Tirado-Rives, *J. Am. Chem. Soc.*, 1996, **118**, 11225–11236.
- 36 C. H. Bennett, *J. Comput. Phys.*, 1976, **22**, 245–268.
- 37 A. Klamt and G. Schüürmann, *J. Chem. Soc., Perkin Trans. 2*, 1993, 799–805.
- 38 J. Andzelm, C. Kölmel and A. Klamt, *J. Chem. Phys.*, 1995, **103**, 9312–9320.
- 39 M. Cossi, N. Rega, G. Scalmani and V. Barone, *J. Comput. Chem.*, 2003, **24**, 669–681.
- 40 V. Barone and M. Cossi, *J. Phys. Chem. A*, 1998, **102**, 1995–2001.
- 41 A. Ben-Naim, *J. Phys. Chem.*, 1978, **82**, 792–803.
- 42 J. A. Keith and E. A. Carter, *J. Chem. Theory Comput.*, 2012, **8**, 3187–3206.
- 43 M. D. Hanwell, D. E. Curtis, D. C. Lonie, T. Vandermeersch, E. Zurek and G. R. Hutchison, *J. Cheminf.*, 2012, **4**, 1–17.
- 44 C. Lee, W. Yang and R. G. Parr, *Phys. Rev. B*, 1988, **37**, 785–789.
- 45 A. Becke, *J. Chem. Phys.*, 1993, **98**, 5648–5652.
- 46 S. Grimme, S. Ehrlich and L. Goerigk, *J. Comput. Chem.*, 2011, **32**, 1456–1465.
- 47 S. Grimme, J. Antony, S. Ehrlich and H. Krieg, *J. Chem. Phys.*, 2010, **132**, year.
- 48 F. Weigend, *Phys. Chem. Chem. Phys.*, 2006, **8**, 1057–1065.
- 49 F. Weigend and R. Ahlrichs, *Phys. Chem. Chem. Phys.*, 2005, **7**, 3297–3305.
- 50 Y.-S. Lin, G.-D. Li, S.-P. Mao and J.-D. Chai, *J. Chem. Theory Comput.*, 2013, **9**, 263–272.
- 51 F. Neese, F. Wennmohs, A. Hansen and U. Becker, *Chem. Phys.*, 2009, **356**, 98 – 109.
- 52 Y. Basdogan, M. C. Groenenboom, E. Henderson, S. De, S. B. Rempe and J. A. Keith, *J. Chem. Theory Comput.*, 2020, **16**, 633–642.

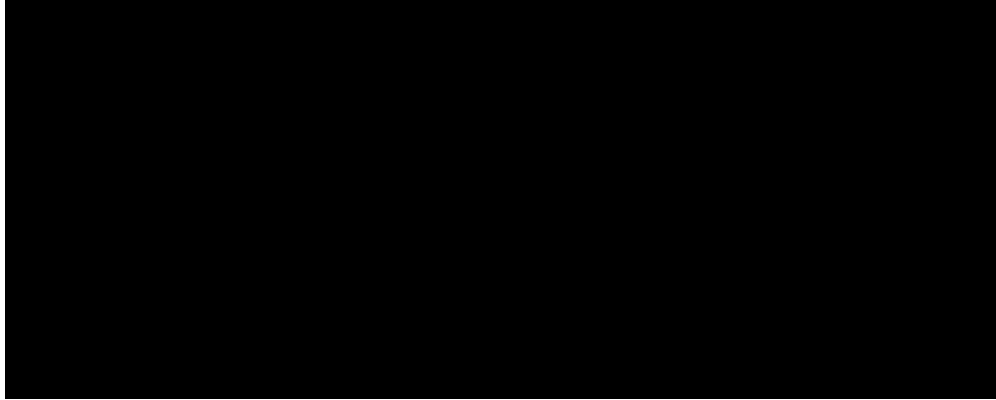
- 53 E. F. da Silva, H. F. Svendsen and K. M. Merz, *J. Phys. Chem. A*, 2009, **113**, 6404–6409.
- 54 J. Lee, B. T. Miller and B. R. Brooks, *Protein Sci.*, 2016, **25**, 231–243.
- 55 C. Bannwarth, S. Ehlert and S. Grimme, *J. Chem. Theory Comput.*, 2019, **15**, 1652–1671.
- 56 S. Genheden and U. Ryde, *Expert Opin. Drug Discovery*, 2015, **10**, 449–461.
- 57 A. Klamt, F. Eckert and W. Arlt, *Annu. Rev. Chem. Biomol. Eng.*, 2010, **1**, 101–122.
- 58 A. Klamt, *Fluid Phase Equilib.*, 2016, **407**, 152–158.
- 59 C. Zhang, C. Lu, Z. Jing, C. Wu, J.-P. Piquemal, J. W. Ponder and P. Ren, *J. Chem. Theory Comput.*, 2018, **14**, 2084–2108.
- 60 A. Cavalli, A. Spitaleri, G. Saladino and F. L. Gervasio, *Acc. Chem. Res.*, 2015, **48**, 277–285.
- 61 J. D. Chodera, D. L. Mobley, M. R. Shirts, R. W. Dixon, K. Branson and V. S. Pande, *Curr. Opin. Struct. Biol.*, 2011, **21**, 150 – 160.
- 62 J. P. Piquemal, L. Perera, G. A. Cisneros, P. Ren, L. G. Pedersen and T. A. Darden, *J. Chem. Phys.*, 2006, **125**, 054511.



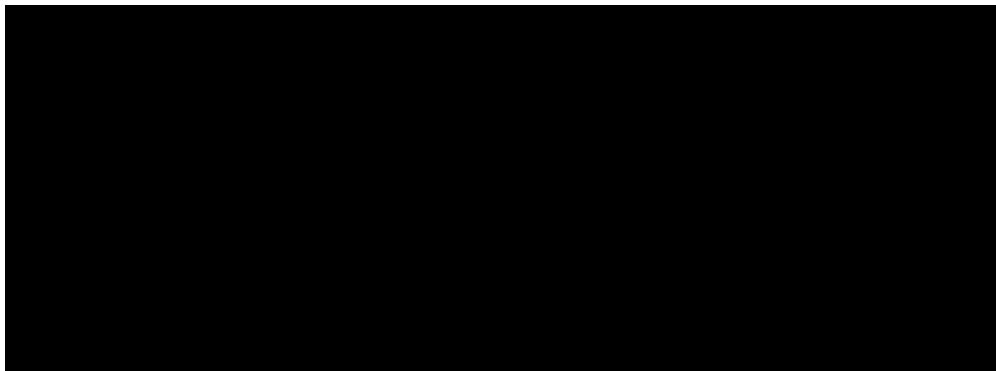


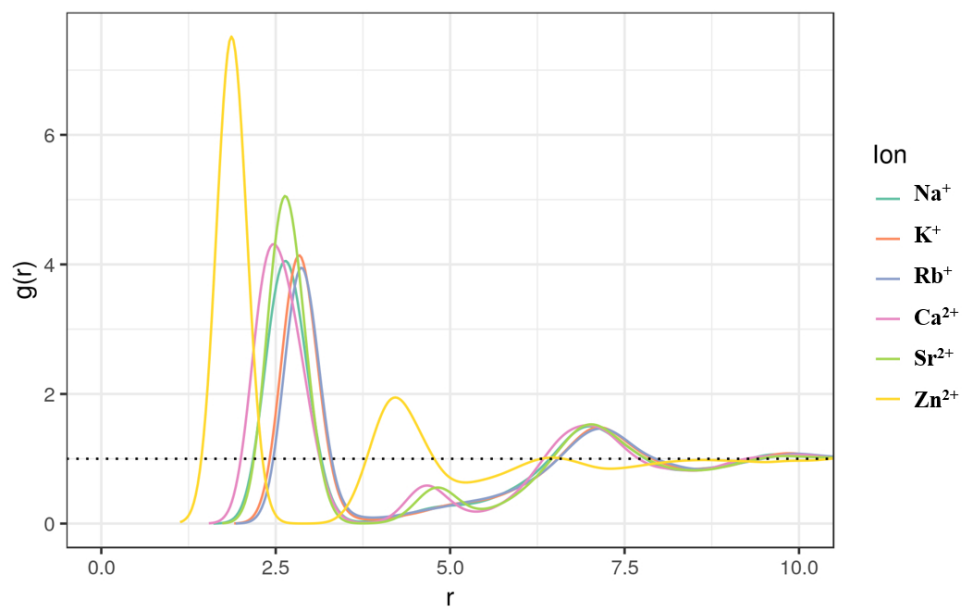


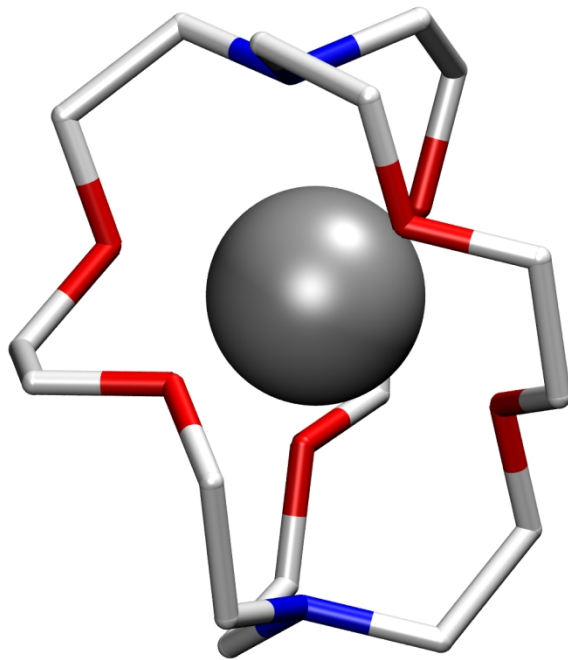




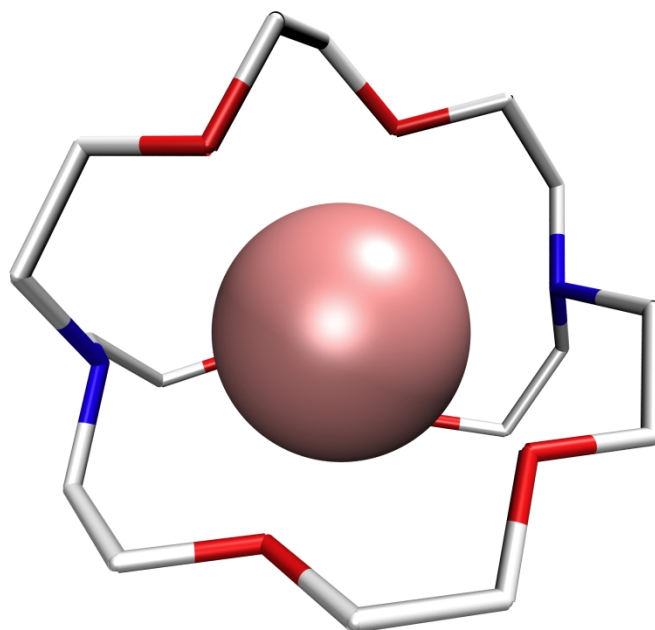




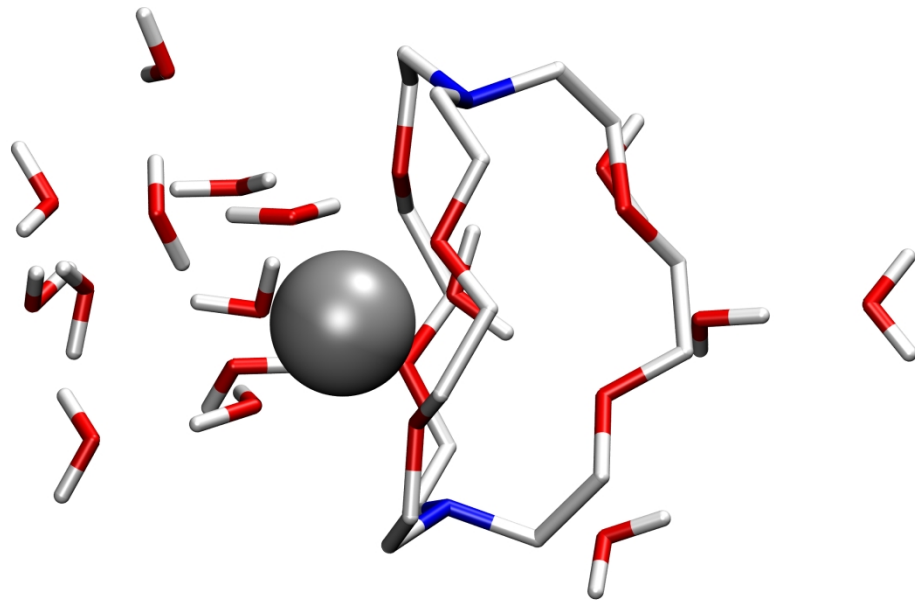




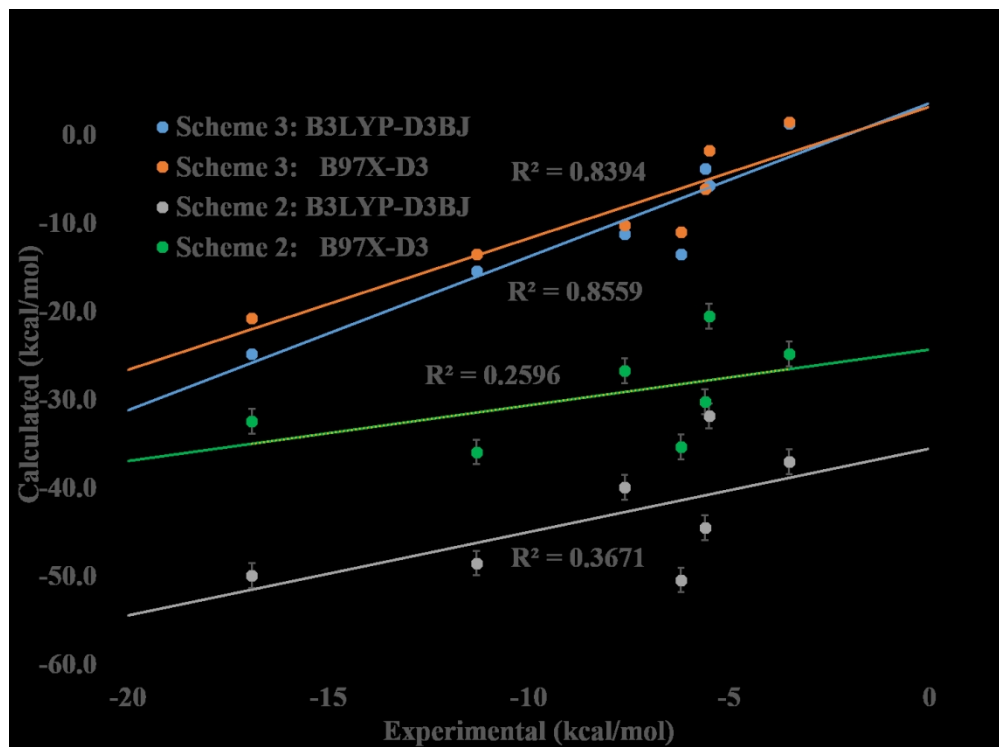
626x600mm (72 x 72 DPI)

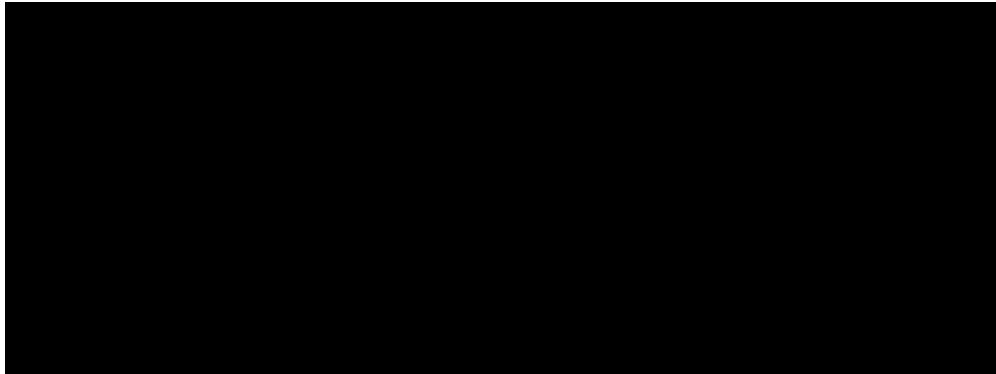


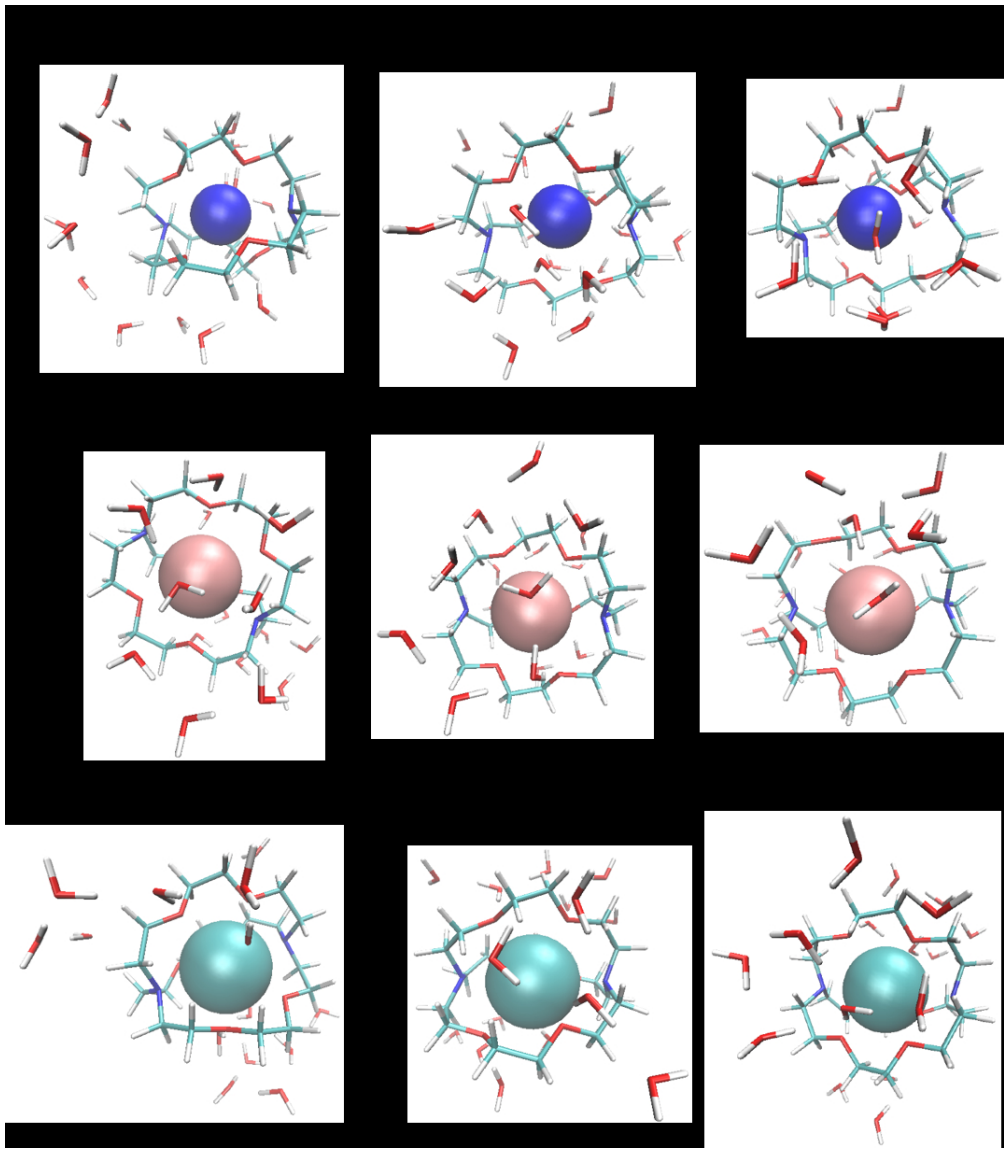
1058x1058mm (72 x 72 DPI)



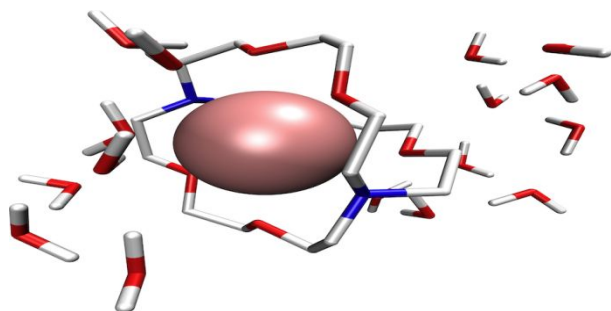
919x817mm (72 x 72 DPI)











Benchmarking quantum chemistry calculation schemes for accurate predictions of absolute stability constants of metal-macrocycle complexes

**Computational predictions of metal-macrocycle  
stability constants require accurate treatments of local  
solvent and pH effects<sup>†</sup>**

Brian M. Gentry,<sup>a</sup> Tae Hoon Choi,<sup>a</sup> William S. Belfield,<sup>b</sup> and John A.

Keith<sup>\*a</sup>

*<sup>a</sup>Department of Chemical and Petroleum Engineering, Swanson School of Engineering,  
University of Pittsburgh, Pittsburgh, PA, USA*

*<sup>b</sup>Department of Chemical Engineering, Loughborough University, Loughborough, UK*

E-mail: [jakeith@pitt.edu](mailto:jakeith@pitt.edu)

# 1 Supporting Information

Figure S1 represents the uncomplexed [2.2.2] and ion-[2.2.2] structures optimized with B3LYP-D3BJ/def2-SVP, but def2-TZVP basis set is applied for the metal ions. Figure S2 shows the three lowest energy structures of Na-, K-, and Rb-[2.2.2] complexes optimized using B3LYP-D3BJ/def2-SVP level of theory, which are used for the binding energy calculations in Scheme 3. Figure S3 represents the three lowest energy structures for the divalent cation complexes, Ca-, Sr-, Zn-, and Pb-[2.2.2] with 16 explicit water molecules optimized with the same method. Figure S4 – S7 show the optimized Cartesian coordinates for the uncomplexed [2.2.2] and ion-[2.2.2] structures. Figure S8 – S14 show the optimized Cartesian coordinates for seven metal-[2.2.2] complexes with 16 water molecules. Each metal complexes has three coordinates.

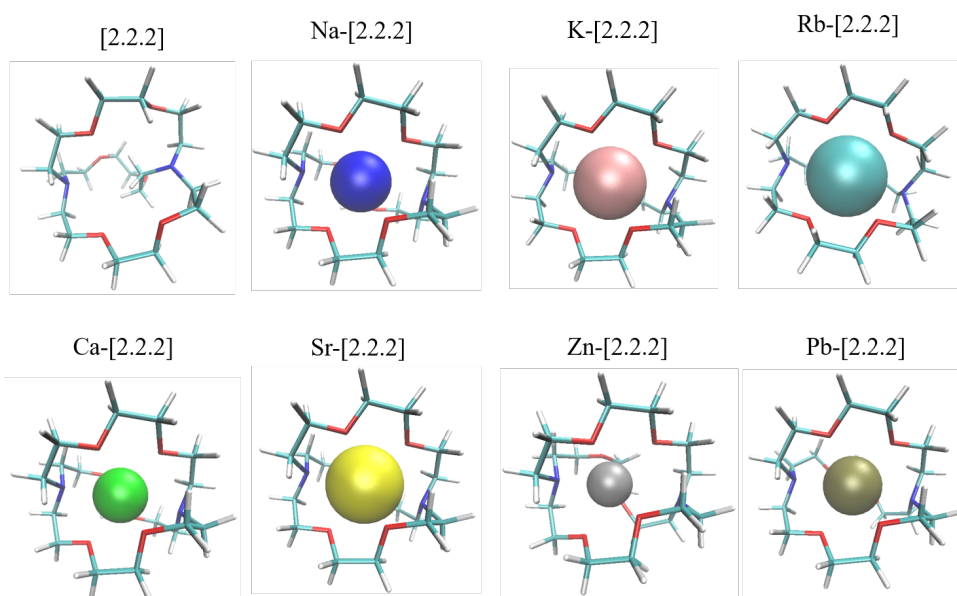


Figure S1: The optimized structures for [2.2.2] and ion-[2.2.2] complexes

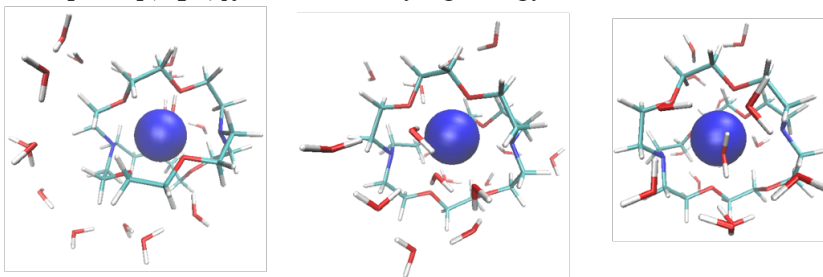
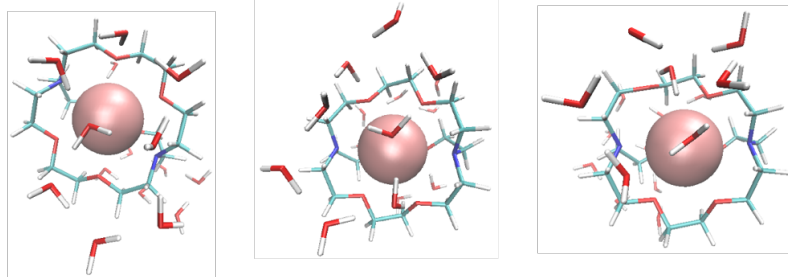
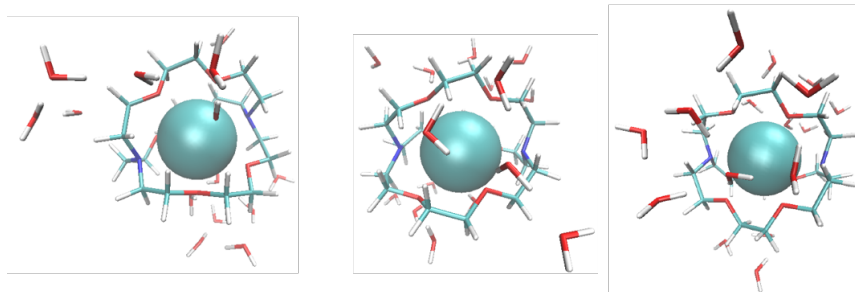
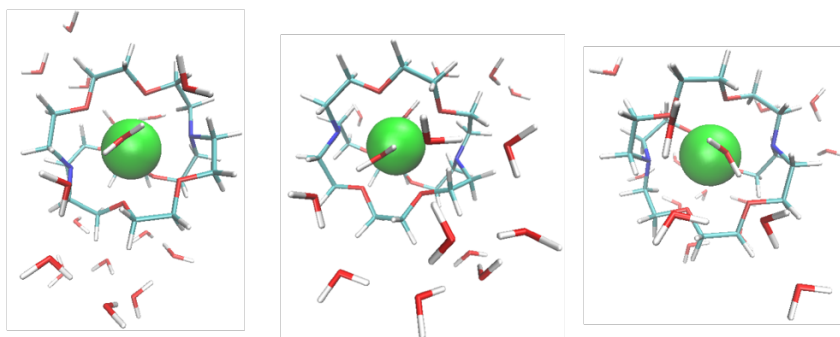
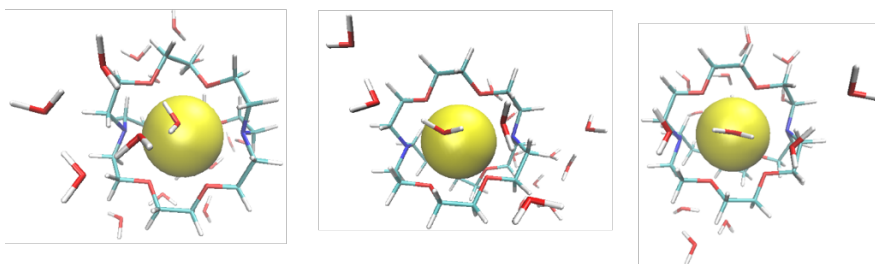
Na-[2.2.2](H<sub>2</sub>O)<sub>16</sub> : Three low-lying energy structuresK-[2.2.2](H<sub>2</sub>O)<sub>16</sub> : Three low-lying energy structuresRb-[2.2.2](H<sub>2</sub>O)<sub>16</sub> : Three low-lying energy structures

Figure S2: Three optimized structures for Na-,K-,and Rb-[2.2.2] complexes with 16 explicit water molecules

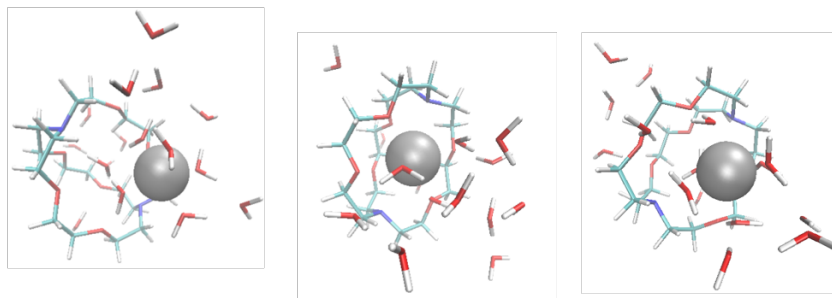
Ca-[2.2.2](H<sub>2</sub>O)<sub>16</sub> : Three low-lying energy structures



Sr-[2.2.2](H<sub>2</sub>O)<sub>16</sub> : Three low-lying energy structures



Zn-[2.2.2](H<sub>2</sub>O)<sub>16</sub> : Three low-lying energy structures



Pb-[2.2.2](H<sub>2</sub>O)<sub>16</sub> : Three low-lying energy structures

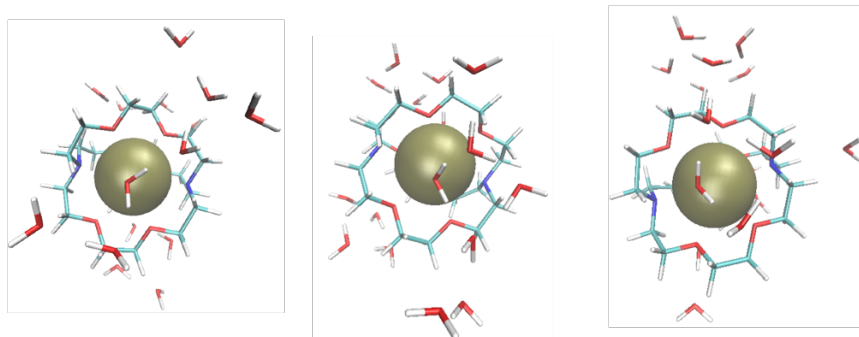


Figure S3: Three optimized structures for Ca-,Sr-,Zn-,and Pb-[2.2.2] complexes with 16 explicit water molecules

62	Coordinates from ORCA-job crypt		
N	-1.54580869867551	3.24756670621938	-0.65872655266461
N	-2.38734518774433	-1.40438577489707	-2.53752424579100
C	-0.48282970498268	2.87867066413639	0.26530805079852
C	0.69384747444496	2.12745728029887	-0.34426713842822
H	-0.90348665309127	2.21861609910341	1.03667516098269
H	-0.07099519979944	3.77105910890158	0.79729536264069
O	0.29746142724775	0.85487686992758	-0.77009857862005
H	1.47619551578998	2.04919580620946	0.44308841238315
H	1.15670504376018	2.68987864276889	-1.17999746368415
C	1.363649982223661	0.03709549427105	-1.18450536961990
C	0.82965969418076	-1.28167840141523	-1.70255000651114
H	2.05137009583268	-0.15503053403389	-0.33273662853056
H	1.95534990010473	0.52652799401562	-1.98572299240463
O	0.45766300582795	-1.14924243853278	-3.05555160352234
H	-0.03110521699862	-1.57742974490423	-1.07659257353735
H	1.61799886232270	-2.05719546370265	-1.59148671723468
O	-0.29843668429536	-2.22481332450381	-3.58336422932785
C	-1.75985823886925	-1.82925752524307	-3.78219669115521
H	-0.23335396423071	-3.10632949449831	-2.91752895695686
O	0.14614618140740	-2.51626666762170	-4.55463344513292
H	-2.29754547089038	-2.69285513523017	-4.21262274493711
H	-1.82171531034210	-1.02785418842315	-4.53575383207830
C	-3.52285229369255	-2.16141277516120	-2.05862149549627
C	-3.50673202058399	-2.42182372529509	-0.54897871386213
H	-3.51782747212838	-3.15385197772614	-2.53729304069641
H	-4.49681363394766	-1.70491914437985	-2.34468264618162
O	-3.53695431472478	-1.26430383588702	0.25898781730702
H	-2.56783238841406	-2.93709312042528	-0.29087242734447
H	-4.35144765415195	-3.09503788598156	-0.28575866158235
C	-4.7789077462746	-0.62255644147144	0.37889297884250
C	-4.56689106890433	0.67700720637004	1.12433958756655
H	-5.49620620674705	-1.25764948200337	0.94102608371913
H	-5.23390131190848	-0.40258140783558	-0.60579937717498
O	-3.94854015976972	1.61546834316012	0.27776562017401
H	-3.92891817075991	0.46855710374568	2.00656381670986
H	-5.53795905619181	1.06430144296153	1.49945969809843
C	-3.44088170595604	2.73292879104723	0.95788713534240
C	-2.75727278644091	3.70503021290234	0.00884964861229
H	-2.74946466556363	2.41163867073699	1.76160156421846
H	-4.26081174002701	3.28671451134205	1.46454435078881
H	-2.56101897797060	4.63490706388279	0.59850140169685
H	-3.49054988387180	3.98211604288369	-0.76474110447797
C	-1.12134672190282	4.2160082823505	-1.66387846434507
C	-1.75024039179064	4.02302293500569	-3.0396263655675
H	-0.03505267533966	4.13769510102119	-1.80827116509842
H	-1.32112557548504	5.25858199419397	-1.32635567739147
O	-1.22895401259421	2.85366664953956	-3.61148516179636
H	-1.50923575188524	4.90521209072821	-3.66615126971253
C	-2.85407378078363	3.98307206185649	-2.94676440694921
H	-1.65522477230707	2.57236646827686	-4.92566806773276
C	-3.10007429374611	2.08600944999157	-5.04964888721311
H	-0.98474233669535	1.78119132872176	-5.29535805831953
H	-1.52412205001820	3.46474131321687	-5.57666230219138
O	-3.33847326855821	0.82985515439031	-4.47564396918483
H	-3.32860824602734	1.99744549310929	-6.12690998702929
H	-3.79893859033169	2.84485913029756	-4.64156838773172
C	-3.52249103222324	0.80297983194950	-3.05705871178231
C	-2.42685501609922	0.04474814842078	-2.31962654990309
H	-3.56453389829284	1.82339337657515	-2.64602589706811
H	-4.51136866605447	0.34545585293289	-2.86522825017848
H	-1.45437703382895	0.46864629640433	-2.59314718433966
H	-2.55001646683155	0.24821900417965	-1.24912289988833
63	Coordinates from ORCA-job na-crypt-b3lyp-opt		
N	-1.40240978337929	2.89412756244158	-0.54090357514957
N	-2.29181393667308	-2.31266794332166	-2.48263600903841
C	-1.21247339636852	2.83698474493492	0.90680405038414
C	-0.04909001579517	1.96135020013914	1.33363396737692
H	-2.12467068155651	2.42293313908359	1.35879101390674
H	-1.06223066266620	3.84751094852709	1.34778396670148
O	-0.20538810614444	0.67103633155802	0.77558425546399
H	-0.02325459581759	1.90932480684335	2.43848834257396
H	0.91727848793998	2.39220381017385	1.01416401438544
C	0.98657034011134	-0.08594259126463	0.77759147082567
C	0.67595193459014	-1.49725239049450	0.35128023701793
H	1.43825532798594	-0.11633139654909	1.78737744597914
H	1.72428952814516	0.36884857951855	0.08747227921796
O	0.04432584322614	-1.48211616338093	-0.91654923991858
H	0.01344555520976	-1.98204791005704	1.09543196157095
H	1.61894635650962	-2.07401390962276	0.31511726245881
C	-0.04011740812184	-2.7737982349833	-1.49421928275658
C	-0.92308840352759	-2.75144213731548	-2.72384482194538
H	-0.41791269382430	-3.49802818596674	-0.74856774779541
H	0.96592347038881	-3.12539166728057	-1.79384965059411
H	-0.89057232828631	-3.77033626569491	-3.1736468057013
H	-0.46098318256919	-2.07137390475125	-3.45563333652769
C	-3.02024601474256	-3.07615325255268	-1.46976194740138
C	-3.01347884296322	-2.42265521317606	-0.08354542233173
H	-2.64373911002539	-4.11410153694094	-1.36822137623542
H	-4.06413154936010	-3.18017566292606	-1.80057326116994
O	-3.31809231064206	-1.04085023275438	-0.10640304066207
H	-2.02693351961476	-2.49048637459471	0.38978766559118
H	-3.72813733975446	-2.96351097361641	0.56688916100739
C	-4.61057146566598	-0.70442612439327	-0.57732721136106
C	-4.86929600319652	0.74708367773430	-0.2488919604636
H	-5.38200533175839	-1.32867430048391	-0.08834157241063
H	-4.68411313449452	-0.85337491303742	-1.66889187711335
O	-3.84898541677885	1.53442677741125	-0.82891714241676
H	-4.87064413920143	0.88751499724486	0.84954895785647
H	-5.86395943030402	1.04212167310327	-0.63698195929985
C	-3.89478944439247	2.88935467374858	-0.43519235004431
C	-2.63261507969220	3.58960273963405	-0.91065751393778
H	-4.00546548659852	2.95567618008752	0.66399456683595
H	-4.77386541750277	3.39864335927025	-0.87494104803417
H	-2.65195005346171	4.63439292202018	-0.53019375220883
H	-2.67791721341062	3.65171528932218	-2.00652962126899
C	-0.23209928017614	3.41724256043726	-1.24123302536726
C	-0.25250363019115	3.15937582513883	-2.73448146375434
H	0.66180712466449	2.92326707752930	-0.84073768287341
O	-0.09691103419728	4.50878709543624	-1.07415827178876
O	-0.34120833438039	1.76542578781942	-2.97728896918569
H	0.67462819514166	3.56560865794134	-3.1809114127820
H	-1.09248574041410	3.68889159860710	-3.21796570274075
C	-0.65357848303182	1.45141209593954	-4.32855850850002
C	-2.15822020666153	1.33270406213146	-4.52391533545576
H	-0.16362561514421	0.49305225816681	-4.55878166667613
H	-0.22896392130362	2.20403499450256	-5.01597539325404
O	-2.67386546628574	0.20712583696937	-3.8352749101857
H	-2.40954458286337	1.28304260050421	-5.59994144846687
H	-2.66463115405272	2.21727150742349	-4.10799593959967
C	-2.59053295569242	-0.99252083062501	-4.58038815624302
C	-3.04311197421939	-2.15936174079096	-3.72507132262441
H	-3.24268527214075	-0.93330447622034	-5.47248666160876
H	-1.56194115047778	-1.15096371120700	-4.9552914012642
H	-4.10030558517142	-1.99607300249453	-3.46820396099397
H	-3.00300192072035	-3.07618189578530	-4.35480756030456
Na	-1.67669435849824	0.35491416525333	-1.29049767867675

Figure S4: The optimized coordinates for uncomplexed [2,2,2] and Na-[2,2,2] complex

63

Coordinates from ORCA-job K-crypt-b3lyp-opt

N	-1.27807271717647	2.99724413064041	-0.49417483332734
N	-2.28999980960465	-2.40695747520008	-2.49795919405604
C	-0.74228327329850	2.86640588252829	0.86496128871083
C	0.44096503618951	1.92268802468621	1.01519314013108
H	-1.54185245141020	2.49274544686211	1.52119215852571
H	-0.43487955460553	3.85510202668812	1.27210867797589
O	0.05228042852875	0.58619377393783	0.75759906769829
H	0.82665171734824	2.01378643887519	2.04928514264653
H	1.27376532743889	2.20388814697341	0.34403133943313
C	1.12542967784715	-0.33384217505074	0.80719379416266
C	0.60774983944879	-1.73862489288082	0.59204700805321
H	1.63347136131599	-0.28771639495511	1.78975097617025
H	1.87312735222069	-0.08834812408550	0.02731798364434
O	0.01248346266481	-1.82544804364118	-0.68897663273686
H	-0.13043612035061	-1.99713165615264	1.37625845068877
H	1.45698459386295	-2.44289507707735	0.68146746800460
C	-0.29086829016851	-3.13680562064530	-1.1188983119519
C	-0.9957377943617	-3.09032032089111	-2.46421726271664
H	-0.90258403307872	-3.66308477878220	-0.36246711649224
H	0.6393309662301	-3.72501223051974	-1.23911001708200
H	-1.08958931617273	-4.13887460588682	-2.82625443527433
H	-0.32032308580973	-2.57712607604400	-3.16655750685864
C	-3.32219199575427	-3.02145397117282	-1.65554984072597
C	-3.47005554538876	-2.42172357039768	-0.25254428425109
H	-3.15990284576778	-4.11318003062561	-1.53546015872719
H	-4.28888810049135	-2.92416836142315	-2.17160060575530
O	-3.68885732611932	-1.02553656912227	-0.21827921515218
H	-2.55992051612426	-2.57797072073814	-0.34184571118972
H	-4.29439482492599	-2.95372144732763	0.26215058311487
H	-4.89286366862666	-0.53654297643509	-0.77214671284844
C	-5.05406465274109	0.89603024393421	-0.30889344615260
H	-5.76048397350758	-1.12660088657406	-0.41805925674297
H	-4.87371020518037	-0.58103800037719	-1.8777555280927
O	-3.94231224237509	1.66352294051081	-0.73743162651526
H	-5.11106735252876	0.90397190139935	0.79576487163032
H	-5.99710218530808	1.3183577843003	-0.70681840692836
C	-3.75485302844263	2.83907506844852	0.02592587720142
C	-2.58848426785896	3.65574396423350	-0.50520511067579
H	-3.61131864620952	2.56616382583677	1.09019905882507
H	-4.65808605326517	3.47868510405782	-0.02544017327632
H	-2.55959321540429	4.60781598509097	0.06821353652162
H	-2.83027683564915	3.92865183091131	-1.54187007969980
C	-0.34484792220906	3.69254833027067	-1.38363469499601
C	-0.59504223436737	3.46097389649760	-2.86272597467272
H	0.67525390874907	3.34362655207524	-1.17149362041073
H	-0.35289727650195	4.78869611371173	-1.19636971475726
O	-0.34408965466574	2.10441430666094	-3.18734172889592
H	0.08043004129215	4.11853476581670	-3.44180569500128
H	-1.62717802441191	3.74470132019974	-3.14101722303746
C	-0.67151484923755	1.76074303454725	-4.52548408090912
C	-2.13386971236813	1.35064576736205	-4.66923953432945
H	-0.00830746450255	0.92889449210140	-4.81077752137394
H	-0.45181383533418	2.59887407453530	-5.21258663079958
O	-2.44438558746811	0.16384607593598	-3.96041007989218
H	-2.39077123920204	1.24101879176572	-5.74051215691190
H	-2.78937709554102	2.13044460122411	-4.25141123398142
C	-2.08398489124951	-1.04398430602188	-4.60504998749631
C	-2.73398445650854	-2.21201461707734	-3.88376421751334
H	-2.45022699107774	-1.03741047254718	-5.64976592839440
H	-0.98349624807432	-1.15716330873106	-4.64663782423937
H	-3.81674590603882	-2.02105691118649	-3.87630522716336
H	-2.57167165916368	-3.12479968504679	-4.49745417864148
K	-1.61818476002579	0.28996866986777	-1.37268858091119

63

Coordinates from ORCA-job Rb-crypt-b3lyp-opt

N	-1.39902047500562	3.13931098164078	-0.51959184499594
N	-2.38167218510751	-2.40224266835054	-2.65613521806431
C	-0.62498723030771	3.05667366208822	0.72120203570606
C	0.55584277850822	2.10124335735006	0.65715470361517
H	-1.28295132147467	2.70442002589475	1.52728571259415
H	-0.24723751140966	4.05362306153440	1.03712860891214
O	0.09370621418079	0.77061117813471	0.51733131662425
H	1.14146622353361	2.20310690368284	1.59129696541242
H	1.23641439241349	2.35247503648135	-0.17892559075564
C	1.12821736961134	-0.19497493037025	0.55698373962178
C	0.53748988609392	-1.58531596442552	0.51502479310827
H	1.71584933451929	-0.08865641125470	1.48917799166038
H	1.82105388363137	-0.05475329573073	-0.29630657330706
O	-0.04272653341717	-1.82595498982702	-0.75374231452416
H	-0.22552585823957	-1.68987941810888	-1.31258229505397
H	1.33889117009299	-2.32077835931637	0.72173523918437
C	-0.69307228729712	-3.080315537418160	-0.84403590157597
C	-1.28815750419432	-3.28713248428669	-2.23405979408936
H	-1.45126282204688	-3.16057789314144	-0.04684629082260
H	0.03678743447619	-3.89588526875047	-0.66945420740342
H	-1.60048675730112	-4.35162722067927	-2.31192031562065
H	-0.45505216370344	-3.15653451775038	-2.94192394669164
C	-3.71479231124680	-2.82054433599176	-2.20516478575648
C	-3.99749694243634	-2.70725193550291	-0.70689903557000
H	-3.93127315133485	-3.87234041323476	-2.50171243867838
H	-4.44910931909345	-2.19347270718853	-2.73352402246405
O	-3.84383419514597	-1.39435161306671	-0.18890239603031
H	-3.33701535467026	-3.36336281496105	-0.12422927530236
H	-5.02585066082380	-3.07053480533056	-0.52761940515214
C	-5.03749130117238	-0.63295826609956	-0.10748599072102
C	-4.77218809418473	0.66197579278796	0.62563726020778
H	-5.80680561936906	-1.19540539437633	0.45400905419685
H	-5.44638321437336	-0.41466037900589	-1.11315205461331
O	-3.99746620279066	1.54252933085694	-0.16951026069797
H	-4.24307729630670	0.43745190664532	1.57291173006886
H	-5.74019912014695	1.13215665876959	0.86627012340930
C	-3.69136242794364	2.75320640526779	0.50349202913200
C	-2.76216295925391	3.64049862461347	-0.31390768031336
H	-3.25399159438384	2.52370891115706	1.49322290491782
H	-4.62236165942206	3.32020084883296	0.69765758554467
H	-2.74869196238685	4.63684115835313	0.18120463236311
H	-3.22616896208213	3.79052257837902	-1.30121581151837
C	-0.69909951699451	3.91338309355911	-1.54885662580199
C	-0.93532904038842	3.44918362914226	-2.97824247295684
H	0.38427975108768	3.84695585933921	-1.37269048239574
H	-0.96296901181171	4.99065349070408	-1.48179336878102
O	-0.29377246605308	2.19814495371779	-3.18436906166043
H	-0.51002789569294	4.20450629162252	-3.66624537709826
H	-2.01980576085562	3.38862305446822	-3.19736551228523
C	-0.19307214986047	1.779096966909587	-4.53438100931587
C	-1.49928971689563	1.23583346531797	-5.10586464075904
H	0.58665614634539	1.00125203020422	-4.55423758017678
H	0.15763760132877	2.61047209316153	-5.17689382437220
O	-2.02667451378224	0.13906238958784	-4.38056066531263
H	-1.33859693627185	0.95987269048999	-6.16635942477886
H	-2.28073081289535	2.01256977242093	-5.08478583535567
C	-1.42665062688050	-1.12601378218668	-4.61926808635132
C	-2.35935786795221	-2.22124556878975	-4.11764298045723
H	-1.26861208696697	-1.26250484743968	-5.70565026123977
H	-0.43440291476229	-1.19543070061598	-4.13191161023258
H	-3.36963056272922	-1.95038061776579	-4.45658968177962
H	-2.09665577950166	-3.16807522509974	-4.63353377281299
Rb	-1.82916952545576	0.31653596935760	-1.50744128265885

Figure S5: The optimized coordinates for K-[2.2.2] and Rb-[2.2.2] complexes

63	Coordinates from ORCA-job ca-crypt-b3lyp-opt	63	Coordinates from ORCA-job sr-crypt-b3lyp-opt
N	-1.50664681018969	2.82483493881902	-0.66601626799272
N	-2.241110173063412	-2.24115552189784	-2.37574946018248
C	-1.54100990839953	2.80190127110850	0.80586604892490
C	-0.42801776858428	1.95253831096427	1.39280770624460
H	-2.50557509812861	2.38278913331545	1.12148044056096
H	-1.47509528754777	3.81936679740616	1.23965706858808
O	-0.37081027415535	0.71269076265755	0.67946654399236
H	-0.62487656073800	1.76272034577828	2.46139336788810
H	0.54906479770543	2.45798694642217	1.32131559071305
C	0.88209046873266	0.03884143688838	0.80789102029094
C	0.69351814520626	-1.39429026878940	0.38632444387529
H	1.23396092958138	0.06023259495006	1.85263208105357
H	1.63404720140879	0.54591596059353	0.17648827790212
O	0.01315225265870	-1.42112385766748	-0.87137690778376
H	0.09407096361192	-1.94617659140115	1.13294976382886
H	1.67644187337528	-1.88730676938279	0.30368853687161
C	0.02034182742008	-2.72386344244930	-1.46677754360586
C	-0.88476082902799	-2.72393553002367	-2.67737024016184
H	-0.30356296714504	-3.46641933733954	-0.71743352045386
H	1.04587519209269	-2.99228403846325	-1.77389145737854
H	-0.89581456423875	-3.74647753520106	-3.10616340682923
H	-0.44059021521309	-2.06768192234677	-3.44102411176788
C	-2.94820609194155	-3.06104481517373	-1.36800751827577
C	-2.97687100138829	-2.39487802788674	0.00691612461025
H	-2.50694781643901	-4.06877907609027	-1.27158862233279
H	-3.97872023465171	-3.22943563385831	-1.71089640127123
O	-3.31368813428153	-1.00777065396249	-0.08367855980603
H	-1.99562202104614	-2.42163882926312	0.49487690356156
H	-3.69054154606491	-2.91485457156101	0.66770156187488
C	-4.66473924020845	-0.72976036127969	-0.46290206499921
C	-4.90274094049644	0.74929809320593	-0.29589182876111
H	-5.36583145062269	-1.29191168260683	0.17532857976056
H	-4.84179576358149	-1.02768581223389	-1.51033382642987
C	-3.86331036510966	1.45794797587425	-0.97371225870845
H	-4.88769936408650	1.02730192637181	0.77317877713351
H	-5.88859072625390	1.01614495436794	-0.71482815975273
C	-3.98696925195554	2.87625447204947	-0.84568115952468
C	-2.66965798455390	3.52194487310983	-1.23743397992140
H	-4.26733317073204	3.11855011492432	0.19316947014952
H	-4.79525238806802	3.24918741085101	-1.49689201303316
H	-2.69945952433189	4.58948054297102	-0.94144324966957
H	-2.57744823946733	3.50046676329271	-2.33221367107200
C	-0.23678957001488	3.36746601664123	-1.17767280894672
C	-0.04946410118731	3.10932745910022	-2.6567746339439
H	0.58921726645486	2.880104058656396	-0.64488234821849
H	-0.14416580102788	4.45483197540345	-0.98586105376204
O	-0.25189810200431	1.71355143776905	-2.90667338277813
H	0.96969097761727	3.40349858768975	-2.95963670160924
H	-0.75296271801171	3.70013806291848	-3.26755894779025
C	-0.39762048799120	1.40112841220011	-4.30034924149805
C	-1.87600801707972	1.26526464217574	-4.59765024658086
H	0.12631527624216	0.45046690589266	-4.48455471844125
H	0.08054065171725	2.16898534200485	-4.92808696828103
O	-2.39904896286303	0.19775589066154	-3.79434861457179
H	-2.06657288413209	1.07602327311303	-5.66599780898106
H	-2.41883463812598	2.18276496897994	-4.32006836304391
C	-2.54837416788050	-1.02318409198414	-4.52830864971487
C	-3.05005587061635	-2.10228828318512	-3.59817356672521
H	-3.27813439296776	-0.87970100594014	-5.34251851231847
H	-1.58627653575628	-1.29674525251342	-4.99667680901982
H	-4.07506993869637	-1.84464354797977	-3.29500316034274
H	-3.10866557291753	-3.05170618787368	-4.16704175921678
Ca	-1.70560179318302	0.30822798651897	-1.37685395287540
N	-1.33563174205924	2.87031320400371	-0.52266005640283
N	-2.36577767879445	-2.28455772838780	-2.44182332669538
C	-1.09319520508168	2.77664968344385	0.92953065540299
C	0.08594773228683	1.89068526148197	1.29148780380686
H	-1.99398127112249	2.35940761275238	1.40329733856929
H	-0.92626576909855	3.77470697346267	1.38178381266114
O	-0.07509922934933	0.61384709931805	0.66725101274011
H	0.13109330899348	1.77262200184349	2.38767875497149
H	1.04514547469221	2.33139482142050	0.97242121728007
C	1.1649396816667	-0.17495501461405	0.66889429247686
C	0.76227409169015	-1.59731029750360	0.31575395714509
H	1.58631941942645	-0.16437629116106	1.66693117616156
H	1.83629297335516	0.24621419085034	-0.05732058681483
O	0.01371052192922	-1.61005174705718	-0.90447386536930
H	0.16014698370572	-2.06193498773838	1.11813932304575
H	1.69029306755059	-2.18234573096480	-0.19800612333411
C	-0.16772571709355	-2.93236907415903	-1.42419119262265
C	-1.03991117343439	-2.88658992341554	-2.66201455580735
H	-0.60226991904241	-3.57772757497416	-0.64020221497095
H	0.81170830042540	-3.36240135305536	-1.69749877007779
H	-1.12293472391412	-3.91870732879771	-3.05822412221407
H	-0.51201489240825	-2.29901757472033	-3.42712513401440
C	-3.21328147909962	-3.04260413041673	-1.49236248462124
C	-3.29055875767936	-2.40903525681094	-0.10363506478997
H	-2.87112457773334	-4.08788612812134	-1.38389457401161
H	-4.22890437821453	-3.11082621720023	-1.90794132149264
O	-3.56170450386393	-1.00629897958250	-0.14800993866811
H	-2.33576510128649	-2.49534468822799	0.43402233839544
H	-4.05523362978181	-2.92590759136066	0.50109509163123
C	-4.86658007484837	-0.59595100806424	-0.55463268539007
C	-5.00406104998706	0.86973998227894	0.20545195300036
H	-5.63973143572280	-1.17531897926452	-0.02302513327812
H	-5.00386480130154	-0.75283167830689	-1.63988604303695
O	-3.88801861866051	1.58239668384991	-0.74892294316829
H	-5.01477505292877	0.99840885568650	0.89151061597255
H	-5.94834502397226	1.26801642520472	-0.61598387974176
C	-3.84500753694857	2.94739967956316	-0.32389824547632
C	-2.57466282042591	3.60861066984368	-0.83054984034389
H	-3.91677714271346	2.98409278704622	0.77761468411530
H	-4.71397134109915	3.49664348957225	-0.72607807723666
H	-2.54327197402231	4.63832825561373	-0.42230677938980
H	-2.64930068812559	3.70561488245129	-1.92327308985037
C	-0.17838962881989	3.45653229918502	-1.22526675713634
C	-0.20047826980308	3.24318119099951	-2.72435865084376
H	0.73622067998172	2.98856994065814	-0.84067968652076
H	-0.08916441684138	4.54234862908081	-1.02194918873833
O	-0.28529297553068	1.84068658433847	-2.99990782237888
H	0.72754395732518	3.65302087714508	-3.15805705824528
H	-1.04264907692957	3.77112349413289	-3.20371932021586
C	-0.48306087991898	1.53915803748202	-4.38879420363040
C	-1.96300604910802	1.32919370536042	-4.64528580537791
H	0.08750577631512	0.62338882499445	-4.60908627503073
H	-0.07576305132596	2.34122199579707	-5.02482433404197
O	-2.42958712774423	0.21489967887755	-3.8718211126167
H	-2.16984922942087	1.16920526608608	-5.71585906424257
H	-2.54340678349833	2.20844945448157	-4.32296558233721
C	-2.48233154401190	-1.01336242400074	-4.60484317190678
C	-3.07183743188821	-2.09238360558121	-3.72381145366578
H	-3.12915070953477	-0.88813388642290	-5.48927720527581
H	-1.47568793399684	-1.27746788141073	-4.97545160022416
H	-4.10982507103378	-1.80860659850260	-3.49688654237556
H	-3.11326321648897	-3.03214853691486	-4.31002961034798
Sr	-1.69763555013453	0.29382967877365	-1.35863481109139

Figure S6: The optimized coordinates for Ca-[2.2.2] and Sr-[2.2.2] complexes



63

Coordinates from ORCA-job zn-crypt-b3lyp-opt

N	-1.65474898203347	2.77463475992493	-0.77555423708877
N	-2.17644411342960	-2.27530990160253	-2.63241292802845
C	-1.80106102247032	2.81041922132999	0.69378531991761
C	-0.76108358745160	1.92680145147557	1.37040831980449
H	-2.80265837466527	2.44800441439864	0.95016025991625
H	-1.71652451278714	3.83885696262493	1.09115123353495
O	-0.60981740588150	0.71724382429718	0.61485265325243
H	-1.07803046301723	1.68258026659836	2.39701174317775
H	0.21352245065620	2.43417865979651	1.43443337660482
C	0.71873348146084	0.17935090782515	0.65466163346684
C	0.68224046732777	-1.22986576554697	0.13591501044769
H	1.08858499842172	0.16969696264913	1.69227189203607
H	1.38237745354239	0.81325181597175	0.04291301363263
O	0.01371099947096	-1.25974301747230	-1.12069192888802
H	0.15405140498102	-1.88656932168307	0.85215891468642
H	1.71626648967426	-1.60407278979885	-2.90819589416620
C	0.10463719972205	-2.56427035181077	-1.71032653052073
C	-0.81316769485225	-2.69709626428233	-2.90819589416620
H	-0.14468100998007	-3.31932520811783	-0.94505496171966
H	1.14718512445682	-2.75465698160721	-2.02049778745185
H	-0.74581964928693	-3.75318300228577	-3.24813111054002
C	-0.42271924796305	-2.08715287961642	-3.7480020161868
C	-2.87196142246300	-2.98730103304496	-1.57159555423206
C	-2.73115388439812	-2.30963951067893	-0.20722141471245
H	-2.52109220956155	-4.03305859881404	-1.46749268960375
H	-3.93862195534453	-3.06400417307534	-1.83298261882575
O	-3.08403661091842	-0.91386656338838	-0.25747992107418
H	-1.70675592758159	-2.34071853620074	0.16724380132120
H	-3.37111209201226	-2.80908635833873	0.53684136483754
C	-4.50221224354430	-0.71352084928489	-0.25112255717797
C	-4.78435377960759	0.75902625322527	-0.13611486090583
H	-4.94789210724238	-1.24589399965843	0.60399536089038
H	-4.94538777946480	-1.12028295352083	-1.17402002320084
O	-3.95759603919093	1.41141044364526	-1.08751521784517
H	-4.54943806696072	1.12831416888584	0.87955708707267
H	-5.85198351443794	0.95337868293621	-0.33923190347672
C	-4.11297171815100	2.82707900979623	-1.12612598425708
C	-2.76958684229575	3.44023643334251	-1.47989416272607
H	-4.46979358522348	3.18535052656494	-0.14630945581789
H	-4.87085505570674	3.11143808293655	-1.87432095672435
H	-2.79496779347544	4.52240437314253	-1.25287648029154
H	-2.59141431817015	3.33388031756698	-2.55904995424981
C	-0.35999658641247	3.35352594437137	-1.19847926096889
C	0.04533905518569	2.85429625101840	-2.56743048857827
H	0.41306128986629	3.05270898657369	-0.48237942378517
H	-0.39631988608376	4.45750304122001	-1.18719424967902
O	0.01733112433646	1.42883390951071	-2.50903359359323
H	1.06205559731092	3.20027179145084	-2.81781082836758
H	-0.63311363789358	3.22191318339748	-3.35451192747601
C	0.04804142257204	0.78211899741473	-3.77662841293973
C	-1.35130664418117	0.75473080408905	-4.36915355265279
H	0.41557040158139	-0.23142419285741	-3.58074684543398
H	0.75227780494970	1.28459976374621	-4.45888257658051
O	-2.27277169329294	0.40865418713359	-3.32233085620206
H	-1.39415186776803	0.01648894876067	-5.18408311549998
H	-1.65359332268379	1.72952958806176	-4.78628749233513
C	-3.38316144602405	-0.42052098680119	-3.71566102327074
C	-2.95293836471207	-1.88518976184777	-3.80036729164039
H	-4.14571222149044	-0.25803512174734	-2.94673288010820
H	-3.78745209785142	-0.05250520153329	-4.67226416439881
H	-3.85198122602045	-2.51121926489203	-3.93761668529724
H	-2.35048019669317	-2.04287593903394	-4.70865052060739
Zn	-1.71850914424506	0.54676999285931	-1.26490000533160

63

Coordinates from ORCA-job pb-crypt-b3lyp-opt

N	-1.67273092306110	3.07342275844668	-0.66271637268033
N	-2.25309354346677	-2.36440523850601	-2.51417549848038
C	-1.26978344187015	3.01490700842537	0.75098110896479
C	0.02554190181851	2.26169997910775	0.98110524079444
H	-2.05817208479297	2.50600442997318	1.32442301383950
H	-1.16337133203401	4.03071520272266	1.18016965613519
O	-0.14529363339762	0.90720633723324	0.55674665533728
H	0.27040253837329	2.28452531433774	2.05727734154279
H	0.87383961838262	2.71800797477893	0.44222957743721
C	0.99912601005320	0.07370411402740	0.74177714073926
C	0.58292958072777	-1.36267984025410	0.53752047263605
H	1.39833124621714	0.19504437767731	1.76343351697884
H	1.78870117056225	0.35932354693451	0.02375191356750
O	-0.03178070914941	-1.48146981269193	-0.74861874992321
H	-0.12883478314374	-1.67967433911587	1.32117906274414
H	1.47460252345423	-2.00875026916150	0.59810024853027
C	-0.08801804221235	-2.81292513485376	-1.26835060233107
C	-0.85040217288370	-2.82716641708203	-2.57570178328167
H	-0.53398420470417	-3.48862268946163	-0.51848186358219
H	0.93688857301563	-3.17418766045323	-1.46285756654721
H	-0.79896634375063	-3.86228566185707	-2.96977842319087
C	-0.32432558566878	-2.18254329633208	-3.29426216928120
C	-3.10017250451072	-3.14283754417712	-1.59385292741624
C	-3.17535916883202	-2.57645217654512	-0.17645397630704
H	-2.77069742486698	-4.19763480186843	-1.52162665958138
H	-4.11704161031984	-3.17614295763695	-2.00951087040345
O	-3.50460598228935	-1.18807893518614	-0.14105874786556
H	-2.21844194165303	-2.65437211695012	0.35193357649161
H	-3.91880226191632	-3.15085450499541	0.40300350421655
C	-4.83409167407606	-0.84818104586848	-0.53034755067670
C	-5.08829973312167	0.57787840310723	-0.10665696774238
H	-5.56137097752702	-1.51199155465198	-0.03335191490583
H	-4.96381526691311	-0.95899787540466	-1.62331433793929
O	-4.08751132700628	1.41711840379230	-0.6852742471097
H	-5.04076750029174	0.65832380845610	0.99406575052549
H	-6.0899865069808	0.89813705488584	-0.44466403004854
C	-4.14896060398640	2.76506315273761	-0.21731804490471
C	-3.04587005727776	3.59414955580858	-0.84168788864545
H	-4.10337018226779	2.76769660160275	0.88641159018230
H	-5.11747261036072	3.21121421661565	-0.5052723490232
H	-3.13774434204753	4.61969841343282	-0.43233246377659
H	-3.22883118541582	3.66238287141185	-1.92389818926374
C	-0.72365065943754	3.86001666031523	-1.48989234779285
C	0.16538292525466	3.01337395377077	-2.38675604188708
H	-0.09036511928339	4.50689023342384	-0.85775040051574
H	-1.29950477140710	4.53382977346160	-2.14023360807841
O	-0.68421910871055	2.17002733858262	-3.15859724113661
H	0.88570125161508	2.39787311197017	-1.81501605367083
H	0.74875271836115	3.68002264629238	-3.04506952176513
C	-0.12739978575306	1.62328803095796	-4.35167034048344
C	-1.22487856613717	0.83469976792536	-5.02481204495015
H	0.73457471473641	0.97254551967487	-4.11331277443897
H	0.22196178214322	2.43021870652828	-5.01953576835064
O	-1.62997483927295	-0.19432650163099	-4.12280410749779
H	-0.85575663842137	0.39200139193081	-5.96592973297215
C	-2.07482363567155	1.50120228904653	-5.25541280052893
C	-2.86598474745654	-0.84644013697646	-4.4122720619346
C	-2.79759090561954	-2.27356580425391	-3.89090970213159
H	-3.69484707811808	-0.28308026625107	-3.93855786018303
H	-3.05736729320982	-0.85926346107155	-5.49815352309728
H	-3.8114569420157	-2.69815522724021	-3.92774213870392
H	-2.18777293021781	-2.88146874369108	-4.57959631954495
Pb	-1.78528687007351	0.36349406477287	-1.46139042455693

Figure S7: The optimized coordinates for Zn-[2.2.2] and Pb-[2.2.2] complexes



Coordinates 1 from ORCA-job K-cryp222-b3lyp-opt			Coordinates 2 from ORCA-job K-cryp222-b3lyp-opt			Coordinates 3 from ORCA-job K-cryp222-b3lyp-opt			
K	-0.04517241330054	-0.18866831432601	K	-0.1020719519563	-0.0721734260825	-0.50053656237962	K	0.68743910082481	-0.2056229357065
N	-0.4703151488416	-1.05124053457118	N	2.65554021940610	0.2233151287518	-0.68419266815573	N	0.51641075712251	-0.3152060846457
O	0.55769575871007	1.90801874675460	O	-3.2998900772050	-0.5707091797305	-0.51348199027052	N	0.6819835948358	-1.12070376642078
C	0.77521104849030	-1.11893037266967	C	3.9590996416052	-0.8113594873478	0.27362029526046	N	1.2898464782350	-0.5771938342081
C	1.93079633789463	-0.39119960265669	C	2.54702640510183	-1.79061143315518	0.842124350662722	C	2.48180662463768	0.20995236570222
H	1.11830475960252	-2.32379649520759	H	2.63758948999040	-0.1927913462382	1.1298603460771	H	0.63588010221590	-0.22729468817780
O	0.62407620489093	-1.3302859307089	O	4.29110044640636	-0.14483929219605	-0.16533833785652	H	1.562394915520376	-1.14462602089117
O	2.16759048087407	-0.42387912997948	O	1.31067609455207	-1.30189159065602	1.3413692925302	C	0.26788976890232	1.2043479305763
H	2.81729743216018	-0.77188476092621	H	3.12070435613202	-2.23930046040995	1.66208772328176	H	0.32652512721997	-0.56891952281405
H	1.76074318503586	0.65035388973878	H	2.56624828262880	-2.57361043262665	0.08960282897175	H	1.83373484511957	-0.14619402700645
C	3.45034968654106	0.04393172689561	C	0.78803800116870	-1.10386921563982	3.24083336387669	C	3.11078146527030	1.76501336551333
C	3.61292683735204	-0.04780318228143	C	-0.58733795561127	-1.5563506704332	2.87850262494056	C	2.79629017056118	2.83761368234221
H	4.2264959597577	-0.59153130613956	H	1.3804006818437	-2.1310573405689	3.2389943281299	H	3.85058551344398	2.25990412377077
H	3.59309717898901	1.02846961487669	H	0.63802923465322	-3.14850288107422	1.39404074111514	H	8.80243321555173	1.0038379625172
O	2.78725293417311	-0.104699142293554	O	-1.57071873651150	-1.6997519151207	1.76402207005277	O	2.24912048215139	0.20804462884551
H	3.33134914387624	-1.08531833224888	H	-0.48109177842240	-0.49324632277166	3.04370309676469	H	0.26541073995545	3.53934781975959
H	3.82556252720277	0.83829154919388	H	-2.79862008946318	-1.04848331365102	2.90584162575922	H	3.58585485541091	3.11051280128469
C	2.7867653047962	0.7705061916550	C	-3.76258746524909	-1.17721405683484	0.92761608902544	C	3.5091611276807	2.4230325420771
C	1.97122907342586	1.89547165697186	C	-5.8905203993720	-0.00300831393770	2.3487417507198	H	8.85825004210370	3.48118175947465
H	2.39245547626719	-0.2312317304539	H	-3.23872592720939	-1.52148179065669	2.245151509263026	H	2.21912839462979	4.00281871163087
H	3.82556252720277	0.83829154919388	H	-4.74190108004200	-0.7584661384390	1.24077910076616	H	7.92776335555830	3.1789272629055
H	2.10898161508075	1.86133421271861	H	-3.9598464640381	-2.24958094849566	0.50759708882811	H	8.33370192041232	2.2837701674988
H	2.4268219330308	-0.2312317304539	H	-3.23872592720939	-1.52148179065669	2.245151509263026	H	8.80243321555173	1.0038379625172
H	2.10898161508075	1.86133421271861	H	-4.74190108004200	-0.7584661384390	1.24077910076616	H	7.92776335555830	3.1789272629055
H	2.4268219330308	-0.2312317304539	H	-3.23872592720939	-1.52148179065669	2.245151509263026	H	8.80243321555173	1.0038379625172
H	2.10898161508075	1.86133421271861	H	-4.74190108004200	-0.7584661384390	1.24077910076616	H	7.92776335555830	3.1789272629055
H	2.4268219330308	-0.2312317304539	H	-3.23872592720939	-1.52148179065669	2.245151509263026	H	8.80243321555173	1.0038379625172
H	2.10898161508075	1.86133421271861	H	-4.74190108004200	-0.7584661384390	1.24077910076616	H	7.92776335555830	3.1789272629055
H	2.4268219330308	-0.2312317304539	H	-3.23872592720939	-1.52148179065669	2.245151509263026	H	8.80243321555173	1.0038379625172
H	2.10898161508075	1.86133421271861	H	-4.74190108004200	-0.7584661384390	1.24077910076616	H	7.92776335555830	3.1789272629055
H	2.4268219330308	-0.2312317304539	H	-3.23872592720939	-1.52148179065669	2.245151509263026	H	8.80243321555173	1.0038379625172
H	2.10898161508075	1.86133421271861	H	-4.74190108004200	-0.7584661384390	1.24077910076616	H	7.92776335555830	3.1789272629055
H	2.4268219330308	-0.2312317304539	H	-3.23872592720939	-1.52148179065669	2.245151509263026	H	8.80243321555173	1.0038379625172
H	2.10898161508075	1.86133421271861	H	-4.74190108004200	-0.7584661384390	1.24077910076616	H	7.92776335555830	3.1789272629055
H	2.4268219330308	-0.2312317304539	H	-3.23872592720939	-1.52148179065669	2.245151509263026	H	8.80243321555173	1.0038379625172
H	2.10898161508075	1.86133421271861	H	-4.74190108004200	-0.7584661384390	1.24077910076616	H	7.92776335555830	3.1789272629055
H	2.4268219330308	-0.2312317304539	H	-3.23872592720939	-1.52148179065669	2.245151509263026	H	8.80243321555173	1.0038379625172
H	2.10898161508075	1.86133421271861	H	-4.74190108004200	-0.7584661384390	1.24077910076616	H	7.92776335555830	3.1789272629055
H	2.4268219330308	-0.2312317304539	H	-3.23872592720939	-1.52148179065669	2.245151509263026	H	8.80243321555173	1.0038379625172
H	2.10898161508075	1.86133421271861	H	-4.74190108004200	-0.7584661384390	1.24077910076616	H	7.92776335555830	3.1789272629055
H	2.4268219330308	-0.2312317304539	H	-3.23872592720939	-1.52148179065669	2.245151509263026	H	8.80243321555173	1.0038379625172
H	2.10898161508075	1.86133421271861	H	-4.74190108004200	-0.7584661384390	1.24077910076616	H	7.92776335555830	3.1789272629055
H	2.4268219330308	-0.2312317304539	H	-3.23872592720939	-1.52148179065669	2.245151509263026	H	8.80243321555173	1.0038379625172
H	2.10898161508075	1.86133421271861	H	-4.74190108004200	-0.7584661384390	1.24077910076616	H	7.92776335555830	3.1789272629055
H	2.4268219330308	-0.2312317304539	H	-3.23872592720939	-1.52148179065669	2.245151509263026	H	8.80243321555173	1.0038379625172
H	2.10898161508075	1.86133421271861	H	-4.74190108004200	-0.7584661384390	1.24077910076616	H	7.92776335555830	3.1789272629055
H	2.4268219330308	-0.2312317304539	H	-3.23872592720939	-1.52148179065669	2.245151509263026	H	8.80243321555173	1.0038379625172
H	2.10898161508075	1.86133421271861	H	-4.74190108004200	-0.7584661384390	1.24077910076616	H	7.92776335555830	3.1789272629055
H	2.4268219330308	-0.2312317304539	H	-3.23872592720939	-1.52148179065669	2.245151509263026	H	8.80243321555173	1.0038379625172
H	2.10898161508075	1.86133421271861	H	-4.74190108004200	-0.7584661384390	1.24077910076616	H	7.92776335555830	3.1789272629055
H	2.4268219330308	-0.2312317304539	H	-3.23872592720939	-1.52148179065669	2.245151509263026	H	8.80243321555173	1.0038379625172
H	2.10898161508075	1.86133421271861	H	-4.74190108004200	-0.7584661384390	1.24077910076616	H	7.92776335555830	3.1789272629055
H	2.4268219330308	-0.2312317304539	H	-3.23872592720939	-1.52148179065669	2.245151509263026	H	8.80243321555173	1.0038379625172
H	2.10898161508075	1.86133421271861	H	-4.74190108004200	-0.7584661384390	1.24077910076616	H	7.92776335555830	3.1789272629055
H	2.4268219330308	-0.2312317304539	H	-3.23872592720939	-1.52148179065669	2.245151509263026	H	8.80243321555173	1.0038379625172
H	2.10898161508075	1.86133421271861	H	-4.74190108004200	-0.7584661384390	1.24077910076616	H	7.92776335555830	3.1789272629055
H	2.4268219330308	-0.2312317304539	H	-3.23872592720939	-1.52148179065669	2.245151509263026	H	8.80243321555173	1.0038379625172
H	2.10898161508075	1.86133421271861	H	-4.74190108004200	-0.7584661384390	1.24077910076616	H	7.92776335555830	3.1789272629055
H	2.4268219330308	-0.2312317304539	H	-3.23872592720939	-1.52148179065669	2.245151509263026	H	8.80243321555173	1.0038379625172
H	2.10898161508075	1.86133421271861	H	-4.74190108004200	-0.7584661384390	1.24077910076616	H	7.92776335555830	3.1789272629055
H	2.4268219330308	-0.2312317304539	H	-3.23872592720939	-1.52148179065669	2.245151509263026	H	8.80243321555173	1.0038379625172
H	2.10898161508075	1.86133421271861	H	-4.74190108004200	-0.7584661384390	1.24077910076616	H	7.92776335555830	3.1789272629055
H	2.4268219330308	-0.2312317304539	H	-3.23872592720939	-1.52148179065669	2.245151509263026	H	8.80243321555173	1.0038379625172
H	2.10898161508075	1.86133421271861	H	-4.74190108004200	-0.7584661384390	1.24077910076616	H	7.92776335555830	3.1789272629055
H	2.4268219330308	-0.2312317304539	H	-3.23872592720939	-1.52148179065669	2.245151509263026	H	8.80243321555173	1.0038379625172
H	2.10898161508075	1.86133421271861	H	-4.74190108004200	-0.7584661384390	1.24077910076616	H	7.92776335555830	3.1789272629055
H	2.4268219330308	-0.2312317304539	H	-3.23872592720939	-1.52148179065669	2.245151509263026	H	8.80243321555173	1.0038379625172
H	2.10898161508075	1.86133421271861	H	-4.74190108004200	-0.7584661384390	1.24077910076616	H	7.92776335555830	3.1789272629055
H	2.4268219330308	-0.2312317304539	H	-3.23872592720939	-1.52148179065669	2.245151509263026	H	8.80243321555173	1.0038379625172
H	2.10898161508075	1.86133421271861	H	-4.74190108004200	-0.7584661384390	1.24077910076616	H	7.92776335555830	3.1789272629055
H	2.4268219330308	-0.2312317304539	H	-3.23872592720939	-1.52148179065669	2.245151509263026	H	8.80243321555173	1.0038379625172
H	2.10898161508075	1.86133421271861	H	-4.74190108004200	-0.7584661384390	1.24077910076616	H	7.92776335555830	3.1789272629055</





Coordinates 1 from ORCA-job ar-cryp222-b3lyp-opt		Coordinates 2 from ORCA-job ar-cryp222-b3lyp-opt		Coordinates 3 from ORCA-job ar-cryp222-b3lyp-opt	
Sr	0.06407394261372	O	0.293549715117342	O	0.43945046440131
N	-2.01267480440141	N	0.578603004150772	N	0.46155556376055
N	1.99679360595338	N	-1.0117419843429	N	-1.74852430612271
C	-2.82343122710995	C	-0.243251782149320	C	-0.15814983291068
C	-3.1709675560831	C	-1.33547891191116	C	-2.37713567495553
H	-2.24637048313177	H	-0.20581255917658	H	0.94988283663528
H	-3.7554161192198	H	2.9225151206340	H	2.13412289891426
O	-2.2488546316776	O	-0.32327135560921	O	-0.09700135566587
O	-1.9848859205716	O	0.70211574650016	O	-1.94894335153032
H	-3.70877439764739	H	1.75441073689902	H	-1.70029015862440
H	-8.33417320235957	H	0.58945320556407	H	-0.46970834445056
C	-2.2488546316776	C	-0.32327135560921	C	-0.20581255917658
C	-0.95313631456063	C	-0.9615054022583	C	-0.9615054022583
H	-2.79258018851107	H	0.04571512242656	H	-3.47676837151313
H	-2.85350733038273	H	-1.12202901961380	H	-1.2202901961380
O	-0.22562220359330	O	-1.44615908394781	O	-1.94587134051531
O	-0.34771591609404	O	-0.213870682081	O	-3.60713710621880
H	-1.18135671875296	H	-1.80195877123559	H	-3.74488445229776
C	0.97125242351127	C	-2.1068871881888	C	-4.83143226584657
C	1.5613920490404	C	-2.8236189475837	C	-2.96458212714264
H	0.14789413917689	H	-1.397489413917689	H	-4.39277448034317
H	0.73391257862314	H	-2.88256625828273	H	-4.56917378384177
H	2.36968280033929	H	-3.4901890990816	H	-6.2222236251031
H	0.7455689894392	H	-3.4645425914031	H	-0.7294858274327
C	3.31289394227548	C	-1.3525132142732	C	-0.31132103186391
C	3.70166476221997	C	-0.13317760789575	C	0.4337238078502
C	3.31117189222330	C	-1.05997900411331	C	-1.43129358021751
H	4.1081668696555	H	-2.186342227929	H	0.23914572201193
H	0.73044692707058	H	0.22386049707058	H	0.66894892707058
H	0.27915936068707	H	0.3196906863070	H	0.55705316816821
H	3.80151591565674	H	-0.3890566762567	H	1.513695537772
H	3.14437176788280	H	-0.2372278689233	H	0.2372278689233
C	2.1048895907771	C	3.1975889917465	C	0.04311608589832
H	4.1297836694500	H	2.1424887386359	H	3.188809400351
H	3.24495294721159	H	2.0344620963227	H	1.8350520485907
H	0.87209143870824	H	0.87209143870824	H	0.8552329156157
H	2.08704147038549	H	3.30021190529094	H	-0.7540536045917
H	2.4544728976698	H	1.16521004007748	H	0.77843966882003
H	0.13355517812951	H	3.794387681146	H	0.13355517812951
H	-3.1757187203955	H	3.3714311067711	H	1.39684764087037
H	-0.31443251565911	H	0.9132465788938	H	-0.44340299606266
H	0.2018682336907	H	4.7765282816498	H	1.02968505257292
H	-2.0699662246386	H	1.4248964537513	H	0.89411550001264
H	-0.171375684749087	H	1.31755684749087	H	2.43482843466554
C	-2.74273114122270	C	1.4862392008776	C	1.96069462418783
H	0.87209143870824	H	0.87209143870824	H	0.8552329156157
H	-3.58006895723272	H	2.1145715254075	H	2.23317695825232
H	-0.2021828648500	H	1.370041008584	H	2.7785017118967
H	-2.3429966224085	H	0.6252215846681	H	0.89411550001264
H	-2.448907667661	H	1.4248964537513	H	0.89411550001264
H	-3.51438667279936	H	-0.3993055786241	H	2.60406491553985
C	-2.5140460161215	C	-2.0344620963227	C	0.8392152552621
H	-1.6172440359617	H	3.794387681146	H	1.74245259918292
H	-0.12198990346364	H	-2.456793371292	H	2.89173452623572
H	0.87410739471245	H	-3.2137677833923	H	1.71316782296580
H	2.04907020518626	H	2.148215858744	H	1.26997891962076
H	0.64419355483939	H	-3.5585899352373	H	2.75183161620090
H	0.4075408890041	H	-4.0751464910159	H	1.0862675828023
H	2.35445056217322	H	1.8364084310465	H	2.1753353563694
H	2.8289777230963	H	3.370879111840	H	1.30004005490197
H	-0.3010554804842	H	2.2553642113966	H	-4.5985071309698
H	-3.8852177533867	H	3.09433706317937	H	-4.45710154959426
H	-3.36380150220897	H	2.148215858744	H	1.26997891962076
H	-3.38048760703239	H	1.7934956240343	H	-7.2610761557272
H	-3.85725198183306	H	1.090232575654	H	-7.7241879479597
H	-3.2055304040405	H	2.148215858744	H	1.26997891962076
H	-3.71417000110227	H	-4.664892870833	H	-0.2564041717150
H	-4.01850615482158	H	-4.1641611282047	H	-1.05634481179499
H	-4.3299311364881	H	-5.4014659433402	H	-1.4137019129482
H	-0.53287342489400	H	2.289943859780	H	-4.2441849270461
H	-2.009330695262	H	1.7702120095216	H	-4.98358776739604
H	-1.52196299146482	H	2.3202281330017	H	-4.5234552547942
H	0.21027591128117	H	0.217825384233	H	2.5730577865032
H	0.7321906576674	H	0.4933193071101	H	3.4731798138193
H	0.06919684612696	H	-0.7484858061639	H	2.70866165203599
H	0.76198768309482	H	1.4387584511670	H	-1.9308521120216
H	1.12719148471817	H	1.2535261501506	H	1.04980079098292
H	1.6377055226800	H	1.44517978582869	H	-2.37630917622184
H	0.35001764244699	H	1.0700788824260	H	-2.26212884209550
H	5.7935518905752	H	0.34163728977067	H	-2.72266406461568
H	0.63005067728091	H	1.7569801984842	H	-2.19501716643717
H	2.85938164888951	H	1.5245680032699	H	-3.47346101914360
H	2.67587781322115	H	2.4685151693834	H	-3.87787613915750
H	3.75267673783400	H	1.4833032698541	H	-3.0787781446592
H	1.64884168839369	H	3.9579394859425	H	-3.71361378833130
H	0.7789449696347	H	3.5818910294449	H	-3.9637165339300
H	1.79475179197171	H	4.0712927003037	H	-4.31012215655956
H	-1.14354516903127	H	-4.87610183890173	H	-0.8489762038757
H	-0.09612338424199	H	-4.9035970675926	H	-0.5073701073543
H	-5.7952077215059	H	-5.7952077215059	H	-0.6702271669914
H	1.7051033860385	H	0.24084946335088	H	4.9697467002464
H	1.76810444748580	H	0.8450141474858	H	5.71422115023331
H	2.14641662134505	H	0.1612149018555	H	4.62897098394210
H	3.62288014242851	H	-2.92780769183615	H	4.0053373668324
H	4.12577527992529	H	-3.55134978217467	H	4.54762420266171
H	2.7143263034718	H	-2.8913864164472	H	4.39638573550492
H	1.10562110324126	H	-2.3823564915314	H	4.83293153563577
H	0.65640026310145	H	-2.78602537655134	H	5.89789215824231
H	1.4224303286196	H	-1.42917001617554	H	5.06334518853770
H	4.00625732721582	H	-0.3226743034828	H	3.84801548194434
H	4.86717562409197	H	-0.1030931168742	H	4.0933031032925
H	4.0255700497489	H	-1.31829913624820	H	3.9179284956941
H	-1.6816050130405	H	-4.09604075301545	H	-3.29272962132345
H	-1.36311964960781	H	-4.42719391039835	H	-2.5186088930044
H	-1.52364510905242	H	-4.82632117562639	H	-4.46139043669287
H	-0.405488911620335	H	-3.25731862811346	H	-2.48072167550852
H	-2.3535422380562	H	-2.97454286816752	H	-0.924628616752
H	-4.7854744399921	H	-3.2635411228614	H	-1.1365889024017

Figure S12: Three optimized coordinates for Sr-[2.2.2] complex with 16 explicit water molecules

Coordinates 1 from ORCA-job zn-crypt22-b3lyp-opt			Coordinates 2 from ORCA-job zn-crypt22-b3lyp-opt			Coordinates 3 from ORCA-job zn-crypt22-b3lyp-opt			
Zn	-1.4109965042525	2.0883471132627	0.15224644127381	4.03112026898318	-0.90497576998282	Zn	3.2652232527075	2.58189862725654	0.21121242415554
N	0.60619278643465	5.50548013518810	1.7064453206000	6.67503461140495	1.8265021069520	N	5.01779523411399	4.00723112562684	3.27922280655624
N	-0.57432634006900	5.1417193266657	-4.02093209963851	4.5923028111919	-2.3186905547182	N	6.85914836558965	4.8397837254508	4.47322108786999
C	0.62840525160432	7.9740937678743	1.17622821969006	8.09100764565672	2.14480136399226	C	5.32294349473238	5.18406403690857	5.40169596211938
H	2.19533021405105	6.8276578649817	0.2167271349424	7.35148140223937	1.4585455460328	H	6.85914836558965	5.68766208960425	4.1376710239996
H	0.83551057544090	7.08971187186332	3.11901129781747	8.1222011536291	2.00301365199762	H	4.19338062059408	5.01193380620096	5.01193380620096
O	1.08246511275848	7.7496873963463	-0.15160109346572	8.3226920529419	0.6773020426194	O	4.47734796831437	6.183955152734	4.93476274870912
H	1.07771539146489	8.91241487042715	1.5632662074494	9.5637353371788	2.2579680325244	H	5.96547759343196	5.60811102846891	6.36225289134409
H	-0.4818698811197	8.1293174136554	1.18978411883514	8.73148140223937	2.6755400532033	H	4.70117801246268	4.38917641947035	5.86917651117567
C	0.86749134077344	8.561213578844	-1.00916037881199	9.16370244555958	8.8244580765178	C	0.51507052582628	6.67698406485256	5.8617624069617
C	1.32797346393504	8.55581517935304	-2.39856018365092	1.16741728697911	-1.0209928970347	C	2.3786776576292	7.34140338101176	5.12980448910056
H	1.38269470122333	7.74801770126358	-0.2368213716032	1.48515801816157	9.89284415054683	H	3.980289152613808	7.4080858670059	6.54785944745560
O	-0.23185070056276	1.01108825128834	-0.99966899214050	-0.08232342904981	8.25711336504307	O	3.12770161735770	5.84242083599944	4.681261063541
O	0.5061039188226	7.58411043133851	-3.0626257330905	-1.94818454786190	-1.3402653749795	O	1.55009118004784	6.3512733649168	4.53157233649168
H	2.37182433899500	8.19207558963307	1.9205183272028	0.898504957123028	9.14420494951894	H	2.76471840805620	6.0312723890285	4.35459871728514
C	1.31290060915225	4.4964040091974	-2.0790857821310	-2.8372286840506	9.1510509876700	C	1.79012439522773	7.48545458960601	5.844405553400
C	1.1121411400512	6.97499019042880	-4.12768750056979	-1.91867152735347	-0.71047201286222	C	0.46576301038374	8.06148780238277	3.8024273623477
C	0.05494802334066	6.1710336807674	-4.86488281786942	-2.6946036310092	5.27106351257675	C	-0.50367341713957	5.84448314073064	3.1977822379437
H	1.38269470122333	8.561213578844	-1.00916037881199	9.16370244555958	8.8244580765178	H	0.86749134077344	7.54999431562369	3.0030751809563
O	0.5061039188226	7.58411043133851	-3.0626257330905	-1.94818454786190	-1.3402653749795	O	-0.3623230396989	5.78916125651143	3.91367225457494
H	2.37182433899500	8.19207558963307	1.9205183272028	0.898504957123028	9.14420494951894	H	1.3909286975406	6.3742516089449	2.9003369406055
C	1.31290060915225	4.4964040091974	-2.0790857821310	-2.8372286840506	9.1510509876700	C	-0.8623230396989	5.1923425369616	4.21630143067078
C	1.1121411400512	6.97499019042880	-4.12768750056979	-1.91867152735347	-0.71047201286222	C	-0.11117910979087	5.2718271143692	0.574225280711
C	0.05494802334066	6.1710336807674	-4.86488281786942	-2.6946036310092	5.27106351257675	C	0.78264903553004	6.44036790999304	0.6026793554100
H	1.38269470122333	8.561213578844	-1.00916037881199	9.16370244555958	8.8244580765178	H	1.1502941412797	5.55987058412616	0.89727376231086
O	0.5061039188226	7.58411043133851	-3.0626257330905	-1.94818454786190	-1.3402653749795	O	1.60231003928259	4.41451860320152	3.04026690942939
H	2.37182433899500	8.19207558963307	1.9205183272028	0.898504957123028	9.14420494951894	H	1.3964496360979	6.10544302439946	0.9047027909571
C	1.31290060915225	4.4964040091974	-2.0790857821310	-2.8372286840506	9.1510509876700	C	0.51507052582628	6.67698406485256	5.8617624069617
C	1.1121411400512	6.97499019042880	-4.12768750056979	-1.91867152735347	-0.71047201286222	C	2.3786776576292	7.34140338101176	5.12980448910056
C	0.05494802334066	6.1710336807674	-4.86488281786942	-2.6946036310092	5.27106351257675	C	3.980289152613808	7.4080858670059	6.54785944745560
H	1.38269470122333	8.561213578844	-1.00916037881199	9.16370244555958	8.8244580765178	H	4.47734796831437	6.183955152734	4.93476274870912
O	0.5061039188226	7.58411043133851	-3.0626257330905	-1.94818454786190	-1.3402653749795	O	1.55009118004784	6.3512733649168	4.53157233649168
H	2.37182433899500	8.19207558963307	1.9205183272028	0.898504957123028	9.14420494951894	H	2.76471840805620	6.0312723890285	4.35459871728514
C	1.31290060915225	4.4964040091974	-2.0790857821310	-2.8372286840506	9.1510509876700	C	1.79012439522773	7.48545458960601	5.844405553400
C	1.1121411400512	6.97499019042880	-4.12768750056979	-1.91867152735347	-0.71047201286222	C	0.46576301038374	8.06148780238277	3.8024273623477
C	0.05494802334066	6.1710336807674	-4.86488281786942	-2.6946036310092	5.27106351257675	C	-0.50367341713957	5.84448314073064	3.1977822379437
H	1.38269470122333	8.561213578844	-1.00916037881199	9.16370244555958	8.8244580765178	H	0.86749134077344	7.54999431562369	3.0030751809563
O	0.5061039188226	7.58411043133851	-3.0626257330905	-1.94818454786190	-1.3402653749795	O	-0.3623230396989	5.78916125651143	3.91367225457494
H	2.37182433899500	8.19207558963307	1.9205183272028	0.898504957123028	9.14420494951894	H	1.3909286975406	6.3742516089449	2.9003369406055
C	1.31290060915225	4.4964040091974	-2.0790857821310	-2.8372286840506	9.1510509876700	C	-0.8623230396989	5.1923425369616	4.21630143067078
C	1.1121411400512	6.97499019042880	-4.12768750056979	-1.91867152735347	-0.71047201286222	C	-0.11117910979087	5.2718271143692	0.574225280711
C	0.05494802334066	6.1710336807674	-4.86488281786942	-2.6946036310092	5.27106351257675	C	0.78264903553004	6.44036790999304	0.6026793554100
H	1.38269470122333	8.561213578844	-1.00916037881199	9.16370244555958	8.8244580765178	H	1.1502941412797	5.55987058412616	0.89727376231086
O	0.5061039188226	7.58411043133851	-3.0626257330905	-1.94818454786190	-1.3402653749795	O	1.60231003928259	4.41451860320152	3.04026690942939
H	2.37182433899500	8.19207558963307	1.9205183272028	0.898504957123028	9.14420494951894	H	1.3964496360979	6.10544302439946	0.9047027909571
C	1.31290060915225	4.4964040091974	-2.0790857821310	-2.8372286840506	9.1510509876700	C	0.51507052582628	6.67698406485256	5.8617624069617
C	1.1121411400512	6.97499019042880	-4.12768750056979	-1.91867152735347	-0.71047201286222	C	2.3786776576292	7.34140338101176	5.12980448910056
C	0.05494802334066	6.1710336807674	-4.86488281786942	-2.6946036310092	5.27106351257675	C	3.980289152613808	7.4080858670059	6.54785944745560
H	1.38269470122333	8.561213578844	-1.00916037881199	9.16370244555958	8.8244580765178	H	4.47734796831437	6.183955152734	4.93476274870912
O	0.5061039188226	7.58411043133851	-3.0626257330905	-1.94818454786190	-1.3402653749795	O	1.55009118004784	6.3512733649168	4.53157233649168
H	2.37182433899500	8.19207558963307	1.9205183272028	0.898504957123028	9.14420494951894	H	2.76471840805620	6.0312723890285	4.35459871728514
C	1.31290060915225	4.4964040091974	-2.0790857821310	-2.8372286840506	9.1510509876700	C	1.79012439522773	7.48545458960601	5.844405553400
C	1.1121411400512	6.97499019042880	-4.12768750056979	-1.91867152735347	-0.71047201286222	C	0.46576301038374	8.06148780238277	3.8024273623477
C	0.05494802334066	6.1710336807674	-4.86488281786942	-2.6946036310092	5.27106351257675	C	-0.50367341713957	5.84448314073064	3.1977822379437
H	1.38269470122333	8.561213578844	-1.00916037881199	9.16370244555958	8.8244580765178	H	0.86749134077344	7.54999431562369	3.0030751809563
O	0.5061039188226	7.58411043133851	-3.0626257330905	-1.94818454786190	-1.3402653749795	O	-0.3623230396989	5.78916125651143	3.91367225457494
H	2.37182433899500	8.19207558963307	1.9205183272028	0.898504957123028	9.14420494951894	H	1.3909286975406	6.3742516089449	2.9003369406055
C	1.31290060915225	4.4964040091974	-2.0790857821310	-2.8372286840506	9.1510509876700	C	-0.8623230396989	5.1923425369616	4.21630143067078
C	1.1121411400512	6.97499019042880	-4.12768750056979	-1.91867152735347	-0.71047201286222	C	-0.11117910979087	5.2718271143692	0.574225280711
C	0.05494802334066	6.1710336807674	-4.86488281786942	-2.6946036310092	5.27106351257675	C	0.78264903553004	6.44036790999304	0.6026793554100
H	1.38269470122333	8.561213578844	-1.00916037881199	9.16370244555958	8.8244580765178	H	1.1502941412797	5.55987058412616	0.89727376231086
O	0.5061039188226	7.58411043133851	-3.0626257330905	-1.94818454786190	-1.3402653749795	O	1.60231003928259	4.41451860320152	3.04026690942939
H	2.37182433899500	8.19207558963307	1.9205183272028	0.898504957123028	9.14420494951894	H	1.3964496360979	6.10544302439946	0.9047027909571
C	1.31290060915225	4.4964040091974	-2.0790857821310	-2.8372286840506	9.1510509876700	C	0.51507052582628	6.67698406485256	5.8617624069617
C	1.1121411400512	6.97499019042880	-4.12768750056979	-1.91867152735347	-0.71047201286222	C	2.3786776576292	7.34140338101176	5.12980448910056
C	0.05494802334066	6.1710336807674	-4.86488281786942	-2.6946036310092	5.27106351257675	C	3.980289152613808	7.4080858670059	6.54785944745560
H	1.38269470122333	8.561213578844	-1.00916037881199	9.16370244555958	8.8244580765178	H</			

Coordinates 1 from ORCA-job pb-cryp222	Coordinates 2 from ORCA-job pb-cryp222	Coordinates 3 from ORCA-job pb-cryp222
Pb 0.196677897371	-0.0136963226087	0.1731644806623
N -0.5400083428057	2.9561793823033	-0.0279042356475
N -1.1723239031567	-2.50370319222985	0.36909061699596
N -1.88305215376582	3.08169514607413	0.56784323994454
C -1.96817110204010	2.64649182650477	-0.06329256975516
H -2.5947551950385	2.4674189684808	-0.01173702760011
H -2.4494841707100	4.1380977866962	0.50303162343262
O -1.47148419022518	1.31936534024231	2.12369958586697
H -3.03952596284726	2.68617120265991	2.324269259928238
H -1.41033650903030	3.32748716776573	2.780646032232697
C -1.32251666195876	0.8461358771313	3.46699430919127
C -1.816095306316	-0.6578624414267	3.46044841578265
H -2.22630620264291	-2.8659863752143	4.07422111159843
H -0.4389432491741	1.3125199774046	3.95362868676518
O -0.0442374285720	-0.04186735822659	2.69227412704295
H -2.02931733313192	-1.2825136942233	3.0217803751988
H -1.04442570160124	-1.00112877513239	4.51054809318347
C 0.04512629432884	-2.4669783709625	2.61034655923541
C 1.25861446382678	-2.8650563672878	1.79236836396576
H 0.90705641567889	-2.8659863752143	2.18777049204045
O 1.6872300780107	-2.88118483204059	3.63686989695732
H 1.41591584900373	-3.06616018871735	1.91147097193395
H 1.21148841279252	-2.3549849376567	2.26383154506377
O 0.28901537505831	-3.42821389821823	-1.77709988020282
C -0.08707826226256	-2.99471986873823	-1.77709988020282
H -0.64452611460858	-3.54141152016031	0.21913267109346
H -0.75451821902130	-2.80542935019779	0.3724203023300333
O 0.87139429881300	-1.80026593265161	-1.697486003390333
H -0.68542495303719	-3.81018214796436	-2.24840466137292
H 0.80079354806159	-2.8169191033210	-2.42489694202309
C 1.33898522030877	-2.951392392117	-2.951392392117
C -2.0334434485822	-3.060698549655	-3.70934015112860
H -2.607338564463	-2.0067516719875	-3.40770712082187
O -0.479101741416	1.53671105161565	1.53671105161565
O -1.11713207266764	0.93570909425845	-2.09809023727270
H -2.9452462680239	-0.0635972395468	-2.08124738537598
H -2.3520107232704	0.4223974900659	-3.70259402319194
H -1.48554663914251	2.30714947435463	-0.44438691189757
C -0.5496864624971	3.2005624718664	-1.47716256100884
H -2.5485799570182	2.4412387351774	-1.9735561995510
H -1.389471745198	2.5917547435463	-3.24902028168137
H -0.84356393509689	4.25776861524120	-1.70436544328578
O 0.49359452047557	3.0627126613240	-1.732044967196901
C 0.4626411187115	3.83286262111995	0.61266230966590
H 1.0256044409206	3.2512986270946	1.813959019218
O 0.1009891872456	4.8159738779181	0.90171922851111
H 1.2429388331156	4.03615752227130	-0.14145746964983
H 1.82282791899267	2.1925103159013	-2.4232494446564
H 0.54238091054409	3.0635780198072	2.69492306578787
H 1.978209154811012	3.3876091851982	2.10453813267186
H 2.25910168709461	1.5038941541786	2.32178981973556
H -1.51721931353867	0.54896201350837	2.70982609413772
C 0.2861145738261	0.99444208371012	3.12575024377641
H 3.38770133242529	2.3104133917489	2.75978291207895
H -0.1416782651541	2.1960265015213	-2.144504056720
H 4.29485202240274	0.028269102374	2.32390490502715
H 4.28612843154418	1.048495255845	0.82813561644213
C 1.45529787770128	3.8529103033109	0.46723175113638
H 4.0136849244084	2.0249491642084	2.0249491642084
H 4.3264850229631	-1.2914794642127	-0.21894782973937
H 1.3798967491712	-0.2754981789644	3.10963531352573
H 3.24299233569629	1.3869582695259	1.3869582695259
H 2.94581148355512	-3.4395331555203	-0.04364979109331
O 2.92615684771742	2.7351437776057	-1.37099620130638
H 0.5335781982137	3.28404405417476	-1.01425263423931
H 2.91016313337408	0.0700585406528	-0.90969146898498
H 1.21779040863185	0.00700585406528	-4.37100181943858
H 1.7971938174672	-0.62011835204198	-4.38191186898956
H 1.52752003899101	0.5732029639246	-5.112953612201
H -2.5195496417709	-2.5195496417709	-4.05152715124900
H 2.64510981874293	-0.192750399615	-4.7279230402637
H 3.4935820317668	-2.8728124164649	3.678135259516957
H -0.44224829122325	1.7257292470466	-0.99851460820174
H -0.58469150987874	0.9656074403381	-0.38551783792358
H -4.9823043011056	1.5016612905127	-1.7158686718087
H 1.951296639852	0.3386147473936	-1.74430368398213
H 2.35920714882848	1.19812054887331	-1.61408199581152
H 1.48524507050121	0.4008831162995	-2.66556954439289
H -1.742419605218187	-0.813266717565213	3.32696107736519
H -4.9300620907868	-1.6237318526457	-0.5387957177113
H -5.42489548730513	-0.16035829784592	0.96691530971197
H -2.10322633856358	-1.2534958367682	0.5889517002404
H -3.0563958554938	-0.9714172224837	0.5853959101476
H -1.98844863814234	-1.64003421089854	-0.33823748628370
H 0.375567823491	1.8259780989327	5.49122105523760
H 2.0263640231430	2.0252973041290	4.80114179647663
C 0.39897805707884	4.1986450988613	0.68349016878465
H 4.444643507216	4.57524006266098	-0.054046979653530
H 6.7920233124272	0.9519217494985	0.9519217494985
H 1.65592325896578	-1.4683849138493	3.85057500440831
H 2.53290532673635	-1.28677849074764	4.4642372685018
H 3.83324204341708	-2.15406954967500	4.31468144904311
H 0.39897805707884	4.1986450988613	0.68349016878465
H 4.444643507216	4.57524006266098	-0.054046979653530
H 6.7920233124272	0.9519217494985	0.9519217494985
H 1.65592325896578	-1.4683849138493	3.85057500440831
H 2.53290532673635	-1.28677849074764	4.4642372685018
H 3.83324204341708	-2.15406954967500	4.31468144904311
H 0.39897805707884	4.1986450988613	0.68349016878465
H 4.444643507216	4.57524006266098	-0.054046979653530
H 6.7920233124272	0.9519217494985	0.9519217494985
H 1.65592325896578	-1.4683849138493	3.85057500440831
H 2.53290532673635	-1.28677849074764	4.4642372685018
H 3.83324204341708	-2.15406954967500	4.31468144904311
H 0.39897805707884	4.1986450988613	0.68349016878465
H 4.444643507216	4.57524006266098	-0.054046979653530
H 6.7920233124272	0.9519217494985	0.9519217494985
H 1.65592325896578	-1.4683849138493	3.85057500440831
H 2.53290532673635	-1.28677849074764	4.4642372685018
H 3.83324204341708	-2.15406954967500	4.31468144904311
H 0.39897805707884	4.1986450988613	0.68349016878465
H 4.444643507216	4.57524006266098	-0.054046979653530
H 6.7920233124272	0.9519217494985	0.9519217494985
H 1.65592325896578	-1.4683849138493	3.85057500440831
H 2.53290532673635	-1.28677849074764	4.4642372685018
H 3.83324204341708	-2.15406954967500	4.31468144904311
H 0.39897805707884	4.1986450988613	0.68349016878465
H 4.444643507216	4.57524006266098	-0.054046979653530
H 6.7920233124272	0.9519217494985	0.9519217494985
H 1.65592325896578	-1.4683849138493	3.85057500440831
H 2.53290532673635	-1.28677849074764	4.4642372685018
H 3.83324204341708	-2.15406954967500	4.31468144904311
H 0.39897805707884	4.1986450988613	0.68349016878465
H 4.444643507216	4.57524006266098	-0.054046979653530
H 6.7920233124272	0.9519217494985	0.9519217494985
H 1.65592325896578	-1.4683849138493	3.85057500440831
H 2.53290532673635	-1.28677849074764	4.4642372685018
H 3.83324204341708	-2.15406954967500	4.31468144904311
H 0.39897805707884	4.1986450988613	0.68349016878465
H 4.444643507216	4.57524006266098	-0.054046979653530
H 6.7920233124272	0.9519217494985	0.9519217494985
H 1.65592325896578	-1.4683849138493	3.85057500440831
H 2.53290532673635	-1.28677849074764	4.4642372685018
H 3.83324204341708	-2.15406954967500	4.31468144904311
H 0.39897805707884	4.1986450988613	0.68349016878465
H 4.444643507216	4.57524006266098	-0.054046979653530
H 6.7920233124272	0.9519217494985	0.9519217494985
H 1.65592325896578	-1.4683849138493	3.85057500440831
H 2.53290532673635	-1.28677849074764	4.4642372685018
H 3.83324204341708	-2.15406954967500	4.31468144904311
H 0.39897805707884	4.1986450988613	0.68349016878465
H 4.444643507216	4.57524006266098	-0.054046979653530
H 6.7920233124272	0.9519217494985	0.9519217494985
H 1.65592325896578	-1.4683849138493	3.85057500440831
H 2.53290532673635	-1.28677849074764	4.4642372685018
H 3.83324204341708	-2.15406954967500	4.31468144904311
H 0.39897805707884	4.1986450988613	0.68349016878465
H 4.444643507216	4.57524006266098	-0.054046979653530
H 6.7920233124272	0.9519217494985	0.9519217494985
H 1.65592325896578	-1.4683849138493	3.85057500440831
H 2.53290532673635	-1.28677849074764	4.4642372685018
H 3.83324204341708	-2.15406954967500	4.31468144904311
H 0.39897805707884	4.1986450988613	0.68349016878465
H 4.444643507216	4.57524006266098	-0.054046979653530
H 6.7920233124272	0.9519217494985	0.9519217494985
H 1.65592325896578	-1.4683849138493	3.85057500440831
H 2.53290532673635	-1.28677849074764	4.4642372685018
H 3.83324204341708	-2.15406954967500	4.31468144904311
H 0.39897805707884	4.1986450988613	0.68349016878465
H 4.444643507216	4.57524006266098	-0.054046979653530
H 6.7920233124272	0.9519217494985	0.9519217494985
H 1.65592325896578	-1.4683849138493	3.85057500440831
H 2.53290532673635	-1.28677849074764	4.4642372685018
H 3.83324204341708	-2.15406954967500	4.31468144904311
H 0.39897805707884	4.1986450988613	0.68349016878465
H 4.444643507216	4.57524006266098	-0.054046979653530
H 6.7920233124272	0.9519217494985	0.9519217494985
H 1.65592325896578	-1.4683849138493	3.85057500440831
H 2.53290532673635	-1.28677849074764	4.4642372685018
H 3.83324204341708	-2.15406954967500	4.31468144904311
H 0.39897805707884	4.1986450988613	0.68349016878465
H 4.444643507216	4.57524006266098	-0.054046979653530
H 6.7920233124272	0.9519217494985	0.9519217494985
H 1.65592325896578	-1.4683849138493	3.85057500440831
H 2.53290532673635	-1.28677849074764	4.4642372685018
H 3.83324204341708	-2.15406954967500	4.31468144904311
H 0.39897805707884	4.1986450988613	0.68349016878465
H 4.444643507216	4.57524006266098	-0.054046979653530
H 6.7920233124272	0.9519217494985	0.9519217494985
H 1.65592325896578	-1.4683849138493	3.85057500440831
H 2.53290532673635	-1.28677849074764	4.4642372685018
H 3.833242043417		



Figure S15 shows the partial charges used in OPLS force field for the molecular dynamics simulations, which are taken from [1].

Atoms	Partial Charge	Atoms	Partial Charge	Atoms	Partial Charge
NT	-0.171	HC	0.128	CT	-0.198
NT	-0.171	CT	-0.198	CT	0.244
CT	-0.198	CT	0.244	HC	0.128
CT	0.244	HC	0.128	HC	0.128
HC	0.128	HC	0.128	OS	-0.405
HC	0.128	OS	-0.405	HC	-0.021
OS	-0.405	HC	-0.021	HC	-0.021
HC	-0.021	HC	-0.021	CT	0.244
HC	-0.021	CT	0.244	CT	0.244
CT	0.244	CT	0.244	HC	-0.021
CT	0.244	HC	-0.021	HC	-0.021
HC	-0.021	HC	-0.021	OS	-0.405
HC	-0.021	OS	-0.405	HC	-0.021
OS	-0.405	HC	-0.021	HC	-0.021
HC	-0.021	HC	-0.021	CT	0.244
HC	-0.021	CT	0.244	CT	-0.198
CT	0.244	CT	-0.198	HC	-0.021
CT	-0.198	HC	-0.021	HC	-0.021
HC	-0.021	HC	-0.021	HC	0.128
HC	-0.021	HC	0.128	HC	0.128
HC	0.128	HC	0.128		

Figure S15: Partial charges for [2.2.2] atoms used in OPLS force field.

## References

- (1) Wipff, G.; Auffinger, P. *J. Am. Chem. Soc.* **1991**, *113*, 5976–5988.